Multiscale streamflow variability associated with El Niño/ Southern Oscillation

MICHAEL D. DETTINGER, DANIEL R. CAYAN, GREGORY J. MCCABE

U.S. Geological Survey, San Diego, California 92093, and Denver, Colorado 80225,USA

JOSÉ A. MARENGO

Instituto Nacional de Pesquisas Espaciais,
CEP 12630-000 Cachoeira Paulista
Sao Paulo - Brazil

***Citation**: Dettinger, M.D., Cayan, D.R., McCabe, G.M., and Marengo, J.A., 2000, Multiscale streamflow variability associated with El Niño/Southern Oscillation, in H.F. Diaz and V. Markgraf, V. (eds.), El Niño and the Southern Oscillation--Multiscale Variability and Global and Regional Impacts: Cambridge University Press, 113-146.*

Abstract

Streamflow responses to the El Niño/Southern Oscillation (ENSO) phenomenon in the tropical Pacific are detectable in many regions. During warm-tropical El Niño and cool-tropical La Niña episodes, streamflows are affected throughout the Americas and Australia, in northern Europe, and in parts of Africa and Asia. In North and South America, correlations between peak-flow season streamflows and seasonal Southern Oscillation Indices (SOIs) show considerable persistence. In South America, correlations between flows in other seasons with December-February SOIs also are notably persistent, whereas, in North America, correlations are smaller when other, non-peak season time periods are considered.

At least two modes of streamflow response to ENSO are present in the Western Hemisphere. When interannual North and South American streamflow variations are analyzed together in a single principal components analysis, two of the leading components are found to be associated with ENSO climate variability. The more powerful of these modes corresponds mostly to ENSO responses by the rivers of tropical South America east of the Andes, along with rivers in southern South America and the southwestern United States, with Brazil experiencing less runoff during El Niños and the other regions experiencing more runoff. This streamflow mode is correlated globally with ENSO-like sea surface temperature (SST) patterns on both interannual and interdecadal time scales; indeed, the tropical South American rivers east of the Andes are coherent with SOI on virtually all historical time scales. The second ENSO-related streamflow mode characterizes other parts of extratropical streamflow variation, emphasizing the north-south differences in streamflows in North America during ENSO extremes and (less robustly) streamflow variations along the central Andes. The relation of this extratropical streamflow mode to ENSO seems to be mostly from scattered interannual time scales and, overall, its decadal variations follow North Atlantic SSTs.

On decadal time scales, the most remarkable variation identified in the Western Hemisphere ENSO-streamflow correlations or teleconnections is a decades-long contrast between the teleconnections of recent decades and teleconnections from about the 1920s into the 1950s. Correlations between streamflows and SOI, Niño-3 SSTs, and even global SSTs nearly vanished

in many regions of North and South America during the earlier period. The change appears to have been associated with weakening of ENSO and, possibly, a weakening of connections between the atmospheric and oceanic components of ENSO during the earlier period. The development of two ENSO-related principal components of North and South American streamflow, rather than one, may be an artifact of the differences in decadal scale responses of streamflows in the tropics and extratropics to multiscale ENSO forcings.

Introduction

Land-hydrologic systems are influenced by climatic changes and human activities on interannual and decadal time scales. A leading mode of global climate variation on interannual time scales is the El Niño/Southern Oscillation (ENSO) of the tropical ocean-air system. The ENSO affects seasonal climate throughout the tropics and in broad swaths of the extratropics, and it thus plays a major role in initiating hydrologic variations in many regions. Ropelewski and Halpert (1987, 1989, 1996) and Kiladis and Diaz (1989) have determined that tropical warm events (El Niños) and cool events (anti-El Niños or La Niñas) influence precipitation and temperatures in many parts of the globe. Depetris and Kempe (1990), Koch et al. (1991), Redmond and Koch (1991), Cayan and Webb (1992), Kahya and Dracup (1993, 1994), Chiew et al. (1994), Moss et al. (1994), Eltahir (1996), Guetter and Georgakakos (1996), Kazadi (1996), Piechota and Dracup (1996), Zorn and Waylen (1997), and Marengo et al. (1998)--among many others--have demonstrated that these ENSO-driven precipitation and temperature fluctuations translate into significant variations of streamflow in several regions of the extratropics. In this chapter, we investigate the relations of streamflow variability to El Niño conditions on global and hemispheric scales.

These interannual climate and hydrologic fluctuations are modulated by, or superimposed upon, lower frequency variations with decadal and longer time scales. The sources of these lower frequency climate variations are uncertain but may have roots in the tropics (Barnett et al. 1992, Trenberth and Hoar 1996), in the extratropical oceans (Pacific: Douglas et al. 1982, Trenberth 1990, Latif and Barnett 1994; Atlantic: Schlosser et al. 1991, Read and Gould 1992, Deser and Blackmon 1993, Tanimoto et al. 1993, Stocker and Broecker 1994, Chen and Ghil 1996; Houghton 1996), or in some interplay of the two (e.g., Graham 1994, Graham et al. 1994, Jacobs et al. 1994). Understanding of precipitation and streamflow variability on these extended time scales is developing (e.g., Probst and Tardy 1987, 1989, Lettenmaier et al. 1994, Marengo 1995, Cayan et al., in review), motivated by the growing realization that extended droughts and periods of repeated flooding are of as much practical importance as ENSO time scale fluctuations and that not all ENSO episodes are alike. In this chapter, we investigate the relative importance of decadal climate variations on Western Hemisphere streamflow variations and show that the leading spatial modes of streamflow variation are related to ENSO processes in ways that vary dramatically on decadal time scales.

As streamflow is the surface hydrological variable most vital for understanding and predicting water supply and water hazards, this chapter focuses on the interannual and longer variations of streamflow associated with ENSO climate forcings, on global and hemispheric scales. After an introductory survey of ENSO influences on the global scale, the chapter focuses on streamflow in North and South America and delineates shared streamflow variations on interannual and decadal time scales that appear in response to ENSO, and ENSO-like (Zhang et al.

1997), climate variability. The dominant ENSO-driven streamflow variations are related to precipitation variations over the Americas, and spatial patterns of Western Hemisphere hydrologic variations associated with ENSO will be characterized by principal component analyses (PCAs) of both streamflow and precipitation. Streamflow variations in the dominant spatial modes are correlated with long-term sea surface temperature (SST) variations in order to identify some of their large-scale climatic underpinnings.

Data

The analyses presented here used instrumental records of streamflow, surface meteorological, atmospheric, and SST variables. The streamflow data either are part of a global collection of monthly streamflow records compiled by the senior author from public domain sources (to be documented elsewhere), or (for South America) are a mix of those public records with private sources provided by coauthor Marengo. In each case, the longest flow records available were used if, on visual inspection and comparisons with neighboring sites, they appeared to be free of large unnatural influences. From the global streamflow set, 732 stations that have more than 15 years of complete streamflow data were used in the next section.

Our North American streamflow analyses in subsequent sections focus mostly on a gridded subset of naturally varying streamflow series of the U.S. Geological Survey Hydroclimatic Data Network (HCDN; Slack and Landwehr 1992). Sites within the conterminous United States with 95% or better data availability for the 60-year period from 1925 to 1984 (to match availability of streamflow data from Canada and South America) were selected for gridding. Some HCDN sites from the central United States were added, despite having somewhat less than 60 years of data, to provide data coverage in that subregion. Canadian streamflow series that met the 95% availability requirement and that appeared to be free from large human-induced changes for the same 60-year period were added to this North American set from public-domain World Meteorological Organization sources. Altogether, 143 sites are included in this North American set. A gridded version of these North American flows was developed by computing the simple (unnormalized) averages of the streamflow series within each 5° x 5° box. The flows were gridded to prevent areas with many sites from overwhelming the pattern analysis, to reduce the influence of missing data points, and to more accurately reflect the degrees of freedom of streamflow variability in North America (see also Lins 1985a, 1985b). Simple averages were gridded to represent total runoff as nearly as possible, rather than weighting small rivers as heavily as large.

The South American streamflow analyses in later sections focus on a 29-site dataset drawn from the global set and proprietary data provided by Marengo (from the Eletrobras and Eletronorte power agencies in Brazil); the series generally span the 62-year period from 1931 to 1992. Because coverage over much of South America was scarce and because several of the flow series represent very large basins (which would not necessarily reflect runoff at the nearest grid point), no gridding was performed for the South American PCA.

For analysis of annual and longer term streamflow variations, monthly streamflow time series like those used here must be summed into yearly totals. These totals need not correspond to calendar years but, rather, often are chosen to distinguish between complete wet seasons by beginning and ending "water years" during the driest months. In this chapter, water years are defined arbitrarily as totals from October though September. This definition is common in North America but is arbitrary when extrapolated to global analyses because, globally, the seasonality of

streamflow hydrographs varies significantly from region to region and hemisphere to hemisphere. Other analyses in this chapter focus on streamflow variations during the time periods of maximum flow in each region. For these analyses, streamflow variations are measured in terms of peak-flow season totals which vary from river to river, but which at each river contain the highest monthly flows in the river's long-term average annual hydrograph.

Global monthly precipitation anomalies for land areas from 1880 to 1992 (Eischeid et al. 1995) and for land *and* sea areas from 1979 to 1995 (Xie and Arkin 1996) were used to describe the hydrologic inputs that drive the streamflow variations considered and to verify those variations. Global SSTs reported by Parker et al. (1995) are a measure of the interannual state of the global climate system, and are analyzed for their association with the streamflow variations considered here. The status of near-surface atmospheric circulations was inferred from monthly sea-level pressure (SLP) anomalies on a near-global, 5° x 5° grid from 42.5°S to 72.5°N, 1951-92, provided by Barnett et al. (1984; with updates since 1984 from the Scripps Institution of Oceanography).

The Southern Oscillation Index (SOI; Fig. 1) is a simple measure of the state of the atmosphere over the tropical Pacific and is a common index of ENSO conditions and effects. The SOI is the difference between deseasonalized, normalized SLP anomalies over Tahiti and Darwin, Australia, and measures the tendency for easterly winds to blow along the Equatorial Pacific. When SOI is positive, easterly winds are strong in the tropics and the tropical Pacific is usually in its La Niña state, with unusually cool SSTs extending westward from the South American coast to the middle of the Pacific basin. When SOI is negative, easterly winds are weak and the tropical Pacific usually is in its El Niño state, with unusually warm SSTs along most of the equator. Seasonal averages of the SOI are considered here in various correlation and composite analyses to map ENSO-induced hydrologic variations. Composites of streamflows in El Niño and La Niña years are obtained by averaging over years in which the SOI is -1 and +1 standard deviations, respectively; correlations use the entire SOI series.

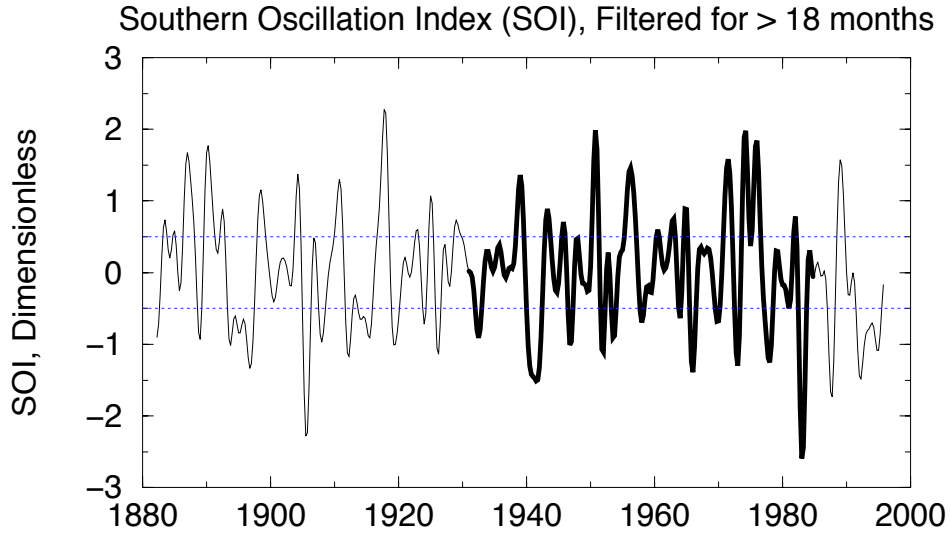

Fig. 1: Southern Oscillation Index (SOI), 18-month moving averaged; heavy during 1931-84 period studied in streamflow principal component analysis.Dashed horizontal lines show SOI = 0.5.

Global ENSO-streamflow relations

In keeping with the global extent of ENSO influences on precipitation and surface temperatures, the effects of El Niños and La Niñas on streamflows also are global. Streamflow series that are correlated with SOI averages for December through February (DJF) at levels significantly different from zero (with $p < 0.05$ by a standard two-side t-test of the sampling errors in correlation estimates; Benjamin and Cornell 1970) are indicated in Figure 2 by colored circles; in the top panel, red-filled circles indicate positive correlations with SOI (so that, at red circles, El Niños correspond to less flow), blue circles indicate negative correlations, and open circles indicate sites at which the correlations are not significant at $p < 0.05$ levels. Underlying the gage symbols in the top panel is a map of the average deviations (from the climatological precipitation totals during non-ENSO DJFs) of DJF precipitation totals during four recent El Niño winters for which global coverage of precipitation series were available from Xie and Arkin (1996). The bottom panel shows deviations of precipitation during three La Niña DJF seasons and the same flow correlations as in the top panel, but with colors reversed so that red circles now indicate dry streamflow responses to La Niña and blue circles indicate wet La Niñas.

Streamflows and precipitation in western North America respond to ENSO with a pattern of dry El Niños in the Northwest and wet El Niños in the Southwest (Cayan and Webb 1992, Kahya and Dracup 1993, 1994). A generally opposite wet-dry pattern typically is associated with La Niñas, but the symmetry is only approximate. El Niños tend to be wetter than normal in more of the southwestern streams, and La Niñas are wetter than normal in more of the northwestern streams, than a strict mirror-image interpretation of the correlations would indicate. The precipitation difference patterns shown in Figure 2a suggest that the wet Southwest El Niño pattern is associated with a large band of higher than average precipitation that reaches from north of Hawaii to the southwestern United States. The tendency for northern and central Mexico also to be deluged by subtropical winter storms during El Niños is evident in the precipitation anomalies of Figure 2a (also, Rogers 1988, and Diaz and Kiladis 1992, Fig. 2.4). During La Niñas, positive precipitation anomalies over the eastern Pacific are diverted farther north and result in a wet Northwest. This influence is seen (Fig. 2b) in the roughly 10° latitude northward shift of precipitation anomalies over the midlatitude eastern Pacific and in higher than normal streamflows in the Pacific Northwest.

In eastern North America, significant positive correlations are observed between winter SOI and many streamflow series (indicating wet La Niñas), except in the extreme Southeast. These correlations reflect wet winters and summers in the Northeast during La Niñas and (less so) dry conditions during El Niños (Fig. 2; Diaz and Kiladis 1992, Kahya and Dracup 1993). The southeasternmost United States is wetter than normal during El Niños in response to a subtropical wet streak across Mexico into the states around the Gulf of Mexico (Piechota and Dracup 1996, Zorn and Waylen 1997).

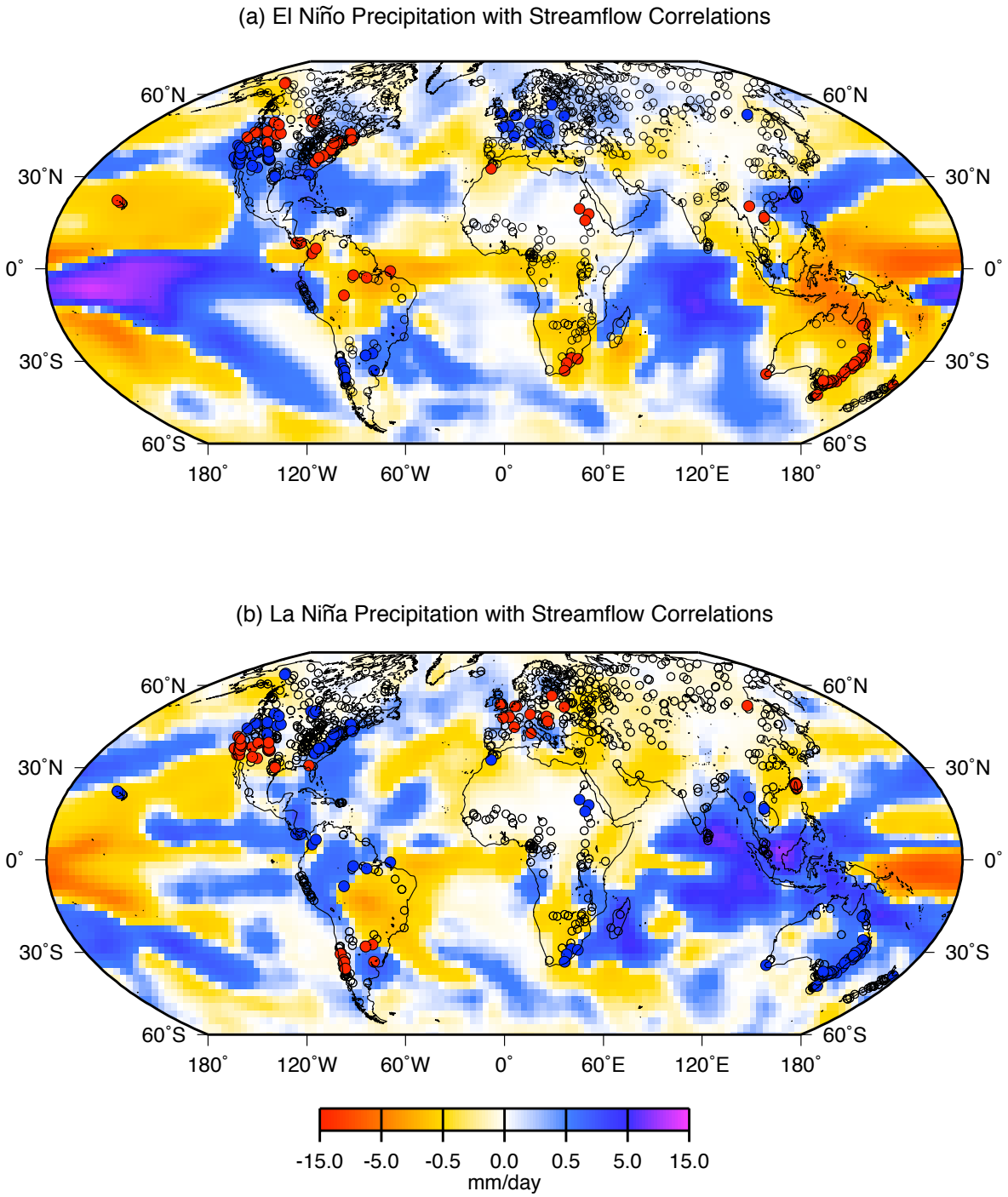

Fig. 2: Differences (shading) between average of October through September precipitation totals during selected El Niño/Southern Oscillation (ENSO) episodes and normal (1979-95) precipitation totals, and significance (circles) of correlations between streamflow totalsfor the same months and December through February Southern Oscillation Index (SOI) for streamflow periods of record. Map (a): Shading indicates average of deviations in El Niño years 1983, 1987, 1992, and 1995 from normal precipitation; red circles indicate streamflow series that are correlated positively with SOI ($p < 0.05$); blue circles are significantly correlated negatively; open circles are not significantly correlated. Map (b): Shading indicates average of deviations in La Niña years 1984, 1985, and 1989 from normal precipitation; color scheme for circles is reversed, with red circles indicatin negative streamflow correlations and blue circles indicating positive correlations.

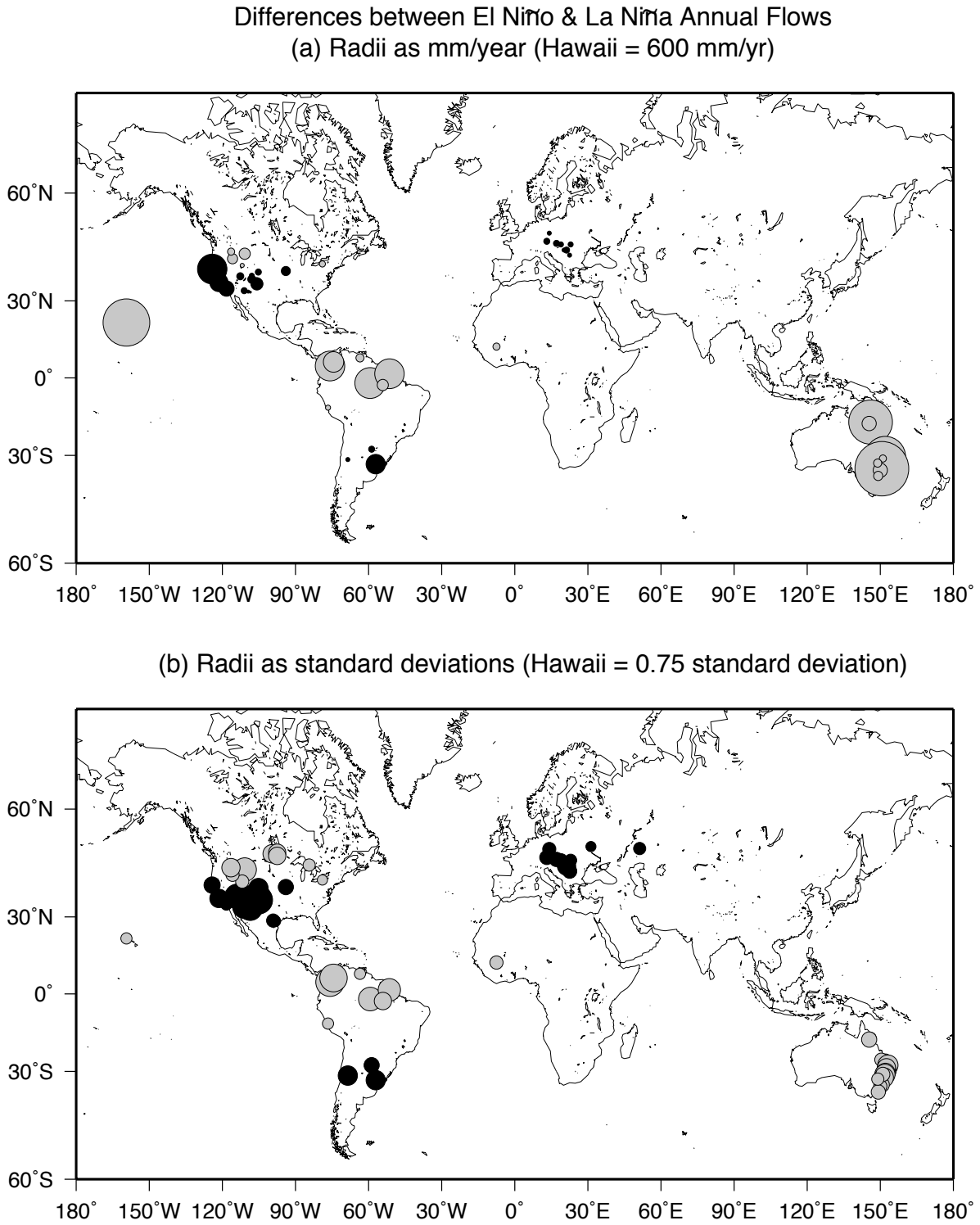

Fig. 3: Significant differences between annual runoff rates in years with positive and negative Southern Oscillation Indices ($p < 0.10$); gray circles indicate drier than normal El Niños, black circles indicate wetter than normal El Niños. Map (a): Radii of circles are scaled to differences in millimeters per year, with the Hawaiian circle representing 600 mm/yr. Map (b): Radii of circles are scaled to differences in local standard deviations of flow, with the Hawaiian circle representing 0.75 standard deviation.

In Central and South America, ENSO influences on streamflow are significant in several regions. Most notably, the Amazon basin (especially in the northern drainages) is drier in terms of both precipitation and flows during El Niño years than during La Niña years (Marengo et al. 1998), whereas Paraguay and Uruguay are wetter than normal in the same years (Rogers 1988, Depetris and Kempe 1990). Central America and northernmost South America also are drier than normal in El Niño years (Rogers 1988, Waylen et al. 1994). We find that the Amazonian and, to a lesser extent, Paraguayan streamflow influences of El Niño are replaced by approximate mirror images during La Niñas. In general, the South American streamflow correlations corroborate the precipitation patterns shown in Figure 2 as well as the less extensive patterns (based on longer precipitation histories) shown by Ropelewski and Halpert (1987, 1989), Kiladis and Diaz (1989), and Diaz and Kiladis (1992). The wet El Niño-dry La Niña precipitation relations of easternmost South America discussed by Rao and Hada (1990), Pisciottano et al. (1994), Enfield (1996), and Diaz et al. (1998) are represented only by small negative correlations in the regions of southeastern Brazil and Uruguay. Along the west coast of South America, precipitation and flows are related to El Niño in a seasonal manner. During both the El Niños and La Niñas composited in Figures 2a and 2b, Peru has been somewhat wet. During boreal summers while El Niños are gaining strength, southern Amazonian and equatorial Pacific precipitations appear to contribute to wet summers and thus to a negative correlation between streamflow and boreal summer SOI (not shown). During DJF, SOI is correlated negatively with Chilean flows (yielding wet El Niños), whereas during the preceding boreal summers, SOI is correlated negatively in southern Chile and positively in northern Chile.

African annual streamflows generally were not well correlated with SOI, except along the Nile and in South Africa (Fig. 2). The Nile River is near the western limit of the Old World limb of the seesaw described by the global SLP variations measured by SOI (Allan et al. 1996), so when SOI is negative (El Niño), pressure over eastern Africa is high and precipitation and streamflow are reduced. Indeed, the occurrence of low flows on the Nile has been used by Quinn (1992) to extend a chronology of El Niño episodes back into the seventh century. In eastern South Africa, low annual flows during El Niños (Fig. 2) are a response to warmer and drier conditions during much of the year leading up to a mature El Niño (Kiladis and Diaz 1989). Early in that year, however, wet conditions prevail (Kiladis and Diaz 1989). The tropical rivers of western Africa experience a complicated regime of wet and dry periods during El Niños and do not yield significant correlations to contemporaneous, seasonal SOIs (Fig. 1; Kazadi 1996). Instead, flows in the rivers are correlated more (not shown) with climate in the equatorial Atlantic and even the North Atlantic.

European streamflows mostly are correlated negatively with winter SOI (indicating wet El Niños), except in Iberia. This streamflow response may correspond to increased winter precipitation, as is weakly suggested by Figure 2a, but Kiladis and Diaz (1989) found no statistically significant El Niño precipitation anomaly in an analysis of longer precipitation records. El Niño mean and La Niña mean streamflow deviations (not shown) indicate that the correlation of European streamflow with SOI comes from El Niños that are wetter than non-ENSO years, especially in east central Europe.

In much of Asia, streamflow correlations with SOI are small or scattered, and no spatial pattern is found in Figure 2. The disturbance of Southeast Asian monsoons by El Niños is evidenced (modestly) by a few positive SOI-streamflow correlations in southeast Asia, whereas higher flows than normal in Taiwan accompany El Niños in response to changes in the western Pacific jet. It is somewhat puzzling that ENSO-related fluctuations of the Indian monsoon (Dhar

and Nandargi 1995) are not evidenced more in the streamflow correlations shown in Figure 1, but records for the subcontinent are short in the present data set, and the use of DJF SOIs may have reduced the significance levels of the relations shown in that figure.

Finally, eastern Australian streamflows respond with low flows to the El Niño droughts on that continent (Nichollis 1992, Chiew et al. 1994). The dry El Niño/wet La Niña patterns are evident in the precipitation anomalies of Figure 1; however, the correlations appear to derive more from wet La Niñas than the dry El Niños, because flows are normally low in many of the rivers and El Niños cannot reduce them as much as wet conditions can enhance them.

Another view of these global streamflow-SOI relations is presented in Figure 3, which shows differences in runoff rates (streamflows/basin area) between boreal winters with low SOIs (El Niño) and high SOIs (La Nina), in mm/yr (Fig. 3a) and in standard deviations (Fig. 3b). The differences are significantly different from zero (by a standard two-sided t-test, Benjamin and Cornell 1970) in Hawaii, western North America, tropical and subtropical South America, eastern Europe, and eastern Australia. As expected, in all cases, the signs of these differences agree with the correlations of Figure 2. When differences between runoff in El Niño and normal years, and between runoff in La Niña and normal years, are mapped as in Figure 3, northwestern and eastern North American, Australian, and European flows responded with larger deviations in El Niño than in La Niña years. Rivers in much of tropical South America respond with flow deviations from normal that are of nearly equal magnitude (but opposite signs) during La Niña and El Niño years, as do the flows of southwestern North America.

In proportion to their long-term averages, streamflow changes in Figure 3 are generally larger than the corresponding precipitation changes. However, such amplifications of precipitation variability in streamflow responses are not uncommon (e.g., Risbey and Entekhabi 1996), and the ENSO responses are an important part of the overall streamflow variability. For each location with significant flow differences shown in Fig. 3b, a corresponding precipitation difference between El Niños and La Niñas was calculated from the 5° x 5° gridded precipitation anomalies of Eischeid et al. (1995). These precipitation differences are compared to the corresponding runoff differences in Figure 4, as fractions of mean flows and precipitation. Overall, the runoff responses shown in Figure 4 are about 4 to 5 times larger than the (gridded) precipitation changes (Fig. 4, Table 1). The most extreme amplifications appear in the semi-arid rivers of Australia and the southwestern United States where flood years dominate the composite streamflow totals.

Table 1 Average fractional differences in precipitation and runoff between El Niño and La Niña episodes this century. Precipitation differences average only over grid cell in Eischeid et al. (1995) that are co-located with streamflow sites in the data set used here.

	Significant differences only ($p < 0.05$)		All differences	
	Precipitation	Runoff	Precipitation	Runoff
Extratropics	+10%	+5%	+6%	0%
Tropics	-9%	-34%	-8%	-16%

Broadly speaking, El Niños tend to yield drier than normal conditions in nearly all of the tropical rivers and a much more spatially varied response among the extratropical rivers. In our global streamflow set, all the tropical flow series that are correlated significantly with SOI are correlated positively with it (representing dry El Niños); when significance levels of the correlations are disregarded, 75% of all the tropical basins are correlated positively with SOI. A

long-term estimate of the zonal averages of El Niño/La Niña tropical precipitation differences over land areas by Diaz and Kiladis (1992, Fig. 2.2) indicates that about 3% less tropical precipitation falls on land during El Niños than during La Niñas (including all tropical land areas). Average extratropical streamflow differences are -0.3% (Table 1), due mostly to widespread cancellation of positive and negative responses at the many extratropical basins.

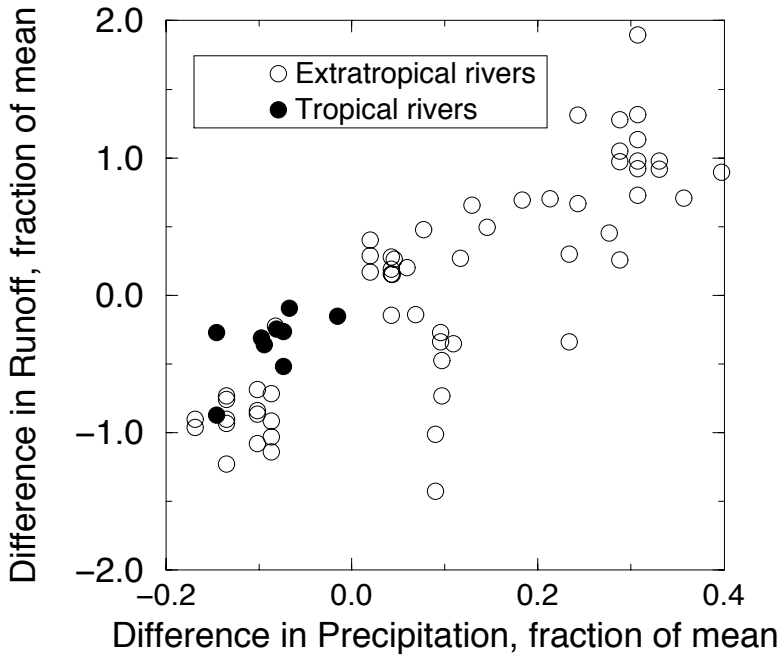

Fig. 4: Differences in runoff values from Fig. 3b and differences in nearest neighbor precipitation values in Eischeid et al. (1995) grid during the same years as percentages of period-of-record mean annual flow and precipitation.

Streamflow-ENSO relations in the Western Hemisphere

To concentrate more on the temporal aspects of SOI-streamflow relations, we focus on interannual streamflow variations in the relatively data-rich Americas in the remainder of this chapter. The North American streamflows used are from the 5° x 5° grid values described earlier, and the South American streamflows are measured rates from 29 sites. Seasonal correlations with SOI and a PCA of these flow series are presented in this section.

Seasonal correlations with SOI

Because, when a significant ENSO-streamflow link exists, El Niños and La Niñas have qualitatively opposite influences on most of the streams, linear correlations of the North and South American flow series with SOI can be used as an approximate shorthand for the separate influences of El Niños and La Niñas on Western Hemisphere flows. Figure 5 shows the correlations between SOI during various seasons and streamflows during each streamflow series' climatological peak-flow season. The correlation patterns of peak-season flows generally do not change much with the season of SOI being considered, although river-to-river differences in the timing of maximum correlations are evident. The long lead and lag correlations between SOI and streamflow arise

because (i) ENSO processes typically develop slowly over months and seasons (e.g., the three-month autocorrelation of SOI is +0.67) and (ii) streamflow series also typically reflect precipitation inputs over several previous months or seasons. Consequently, by June through August (JJA) of the year preceding maturation of an El Niño--which is JJA of year 0 in the terminology of Rasmusson and Carpenter (1982)--the correlations between SOI and the following year's peak-season streamflows already have been established in many regions. As can be expected from the previous section and from studies listed there, flow in the Amazon basin, northernmost South America, and northwestern North America are correlated positively with DJF SOI; peak-season flows in southwestern and southeastern North America are correlated negatively with DJF SOI. (The strengths of the correlations mapped in Figure 5 differ from those indicated in Figure 2 because, in Figure 5, only peak-season flow variations are considered.)

Another way of viewing these correlations is in a tabular form, such as in Figure 6, intended to make the temporal evolution of SOI influences more obvious. Because of the relatively slow (interseasonal to interannual) pace of ENSO dynamics, most of the streamflows that correlate well with SOI maintain correlations with the same signs throughout the six seasons shown in each panel, and most of the significant correlations remain significant from the preceding summer through at least the DJF of the mature El Niño or La Niña. In northern North America, peak-season streamflows (typically spring or summer) are correlated most with winter and spring SOI; farther south in North America, peak flows tend to correlate best with preceding autumn and winter SOIs. In South America, peak flows show maximum correlations with SOI in austral winter and spring in the northern tropical regions (top of right-hand panel of Figure 6) and in austral summer and fall just south of the equator (e.g., Rio Negro, Brazil). In the far south, peak flows show maximum correlations with SOI as it develops towards ENSO episodes in the preceding austral winter in Argentina on the east side of the Andes and in the subsequent winter in Chile on the west. In the extratropics, only the peak-season flows typically are well correlated with DJF SOI. In tropical South America east of the Andes, flows from most of the 18-month period shown are well (and positively) correlated to DJF SOI; along the Peruvian coast, correlations are less pronounced on these time scales (and for a shorter period of record, 1930s to 1960s) and of the opposite sign from the other rivers in tropical South America.

Principal components of North and South American streamflow

The large regions of persistently significant correlations of similar signs in both the North American and South American panels of Figure 6 indicate that flow on both continents varies together with SOI (and the ENSO dynamics) on interannual time scales and that those variations are organized on at least a hemispheric scale. The correlation patterns shown so far have represented long-term average streamflow responses to ENSO with no guarantees that those patterns of ENSO responses have occurred repeatedly. Determining the relative importance and reproducibility of these ENSO-driven streamflow patterns from episode to episode requires a more detailed analysis. One method for representing the most commonly occurring patterns within time-varying fields of scalar quantities (like streamflow) is spatial PCA (see, e.g., Manly 1986, Barnston and Livezey 1987). This method computes a set of spatial patterns, or basis functions, that in linear combinations can be used to describe all variability in a set of concurrent time series. The patterns obtained from PCA are particularly useful because they are, by design, the patterns which can represent the maximum fractions of the variability using the fewest patterns. They are obtained by standard matrix manipulations to obtain the eigenvectors of the spatial cross correlation matrix of

the time series. These eigenvectors are the desired spatial basis functions (spatial patterns) and are called empirical orthogonal functions (EOFs). The strength of a particular EOF pattern in the original time series each year forms a time series called the principal component (PC) series, which is obtained by projecting the original time series onto that EOF. The initial EOF patterns are optimal for representing the collection of time series as a whole but typically do not distinguish between regions that vary together and those that have different time histories. For our purposes then, a useful "natural" division of the streamflow series into regions of shared variability was developed by "rotating" (Richman 1986) the EOFs and PCs to maximize the spatial variance of the EOF patterns. This rotation typically yields spatial basis functions (the rotated EOFs--REOFs) that delineate regions in which significant temporal variations are shared (or are in consistent contrast). Lins (1985a, 1985b) has applied rotated PCA to streamflows in the conterminous United States and provides a discussion of the steps, limitations, and usefulness of this method for characterizing regional flow variability.

Because the discussion so far and the correlations in Figure 6 suggest that ENSO-correlated variations will be a mode of streamflow variability that is shared in broad areas of the Western Hemisphere, a spatial PCA was performed on the year-to-year streamflow variations from both continents. The PCA separated the streamflow variations into natural, uncorrelated modes, some of which were expected to be ENSO responses and others of which were likely to be interannual variations of (mostly) unknown origins. The PCA-identified modes of streamflow variation were analyzed by various correlations to identify those modes linked to ENSO and to determine the nature of those links.

Briefly, the PCA was done as follows: The common period of record for most of the streamflow series (1931-84; Fig. 1) was extracted from each series, and the annual flow cycle (which varied substantially from series to series, as in Fig. 5d) was removed by low-pass filtering each series with a linear filter (Kaylor 1977) with a half-power point at $(18 \text{ months})^{-1}$. Without this filtering, the differences in annual hydrographs from place to place dominated the analysis; also, Trenberth (1984) has shown that, in analyses related to the SOI, significant signal-to-noise improvements are provided by such filtering. Next, a standard EOF analysis of the cross-correlation matrix of the flow series was performed to obtain orthogonal EOFs and PCs. The eigenspectrum of the correlation matrix was inspected, and the number of PCs (6) that captured more variance than components of the noise background was estimated according to the ad hoc rules for sampling errors suggested by North et al. (1982). These six modes then were rotated by an orthogonal Varimax procedure (Richman 1986) to obtain rotated PCs (RPCs) that depict distinct but nonorthogonal indices of flow variability. The spatial patterns associated with these modes of flow variation are characterized here by the temporal correlation coefficients of the flow series with respect to the RPC time series.

The leading six components of (North and South) American streamflow variability constitute 47% of the interannual streamflow variance. In this chapter, however, only two RPCs (numbers 2 and 5 from among the six significant components) are of interest because together they appear to reflect regional ENSO responses by streamflow in the Americas; the other modes are discussed elsewhere (e.g., Dettinger and Cayan, 1998). The spatial pattern (REOF) and temporal progression (RPCs) of the first such component, RPC 2, which captures 9.0% of interannual streamflow variance, are shown in Figure 7. The spatial pattern includes the opposition of flow variations between the rivers of tropical and southern South America and, less prominently, between the southern United States and the northwestern and eastern United States. The RPC 2 dips to notably negative values in 1933, 1940-42, 1947, 1958, 1966, 1970, 1973, and 1983; all are

associated with El Niño episodes in the tropical Pacific. Positive excursions of this mode are notable in 1936, 1939 (La Niña), 1945, 1950 (La Niña), 1963, 1972, 1974 (La Niña), and 1976 (La Niña), only half of which are La Niña episodes. Figure 8 shows how this ENSO-related RPC, and another, vary with SOI and Niño-3 SST (defined as the mean SST anomaly in the region from 5°S to 5°N, and from 150°W to 90°W). The four points in the lower left corner of Figure 8a are seasonal conditions and responses from the large El Niño of 1982-83. The correlation between the first ENSO streamflow mode (RPC 2) and SOI ($r = 0.67$; Fig. 8a) clearly is improved by the 1983 warm event but, even without that event, a linear relation between SOI and RPC 2 remains ($r = 0.61$ when the 1983 points are removed). The relation between RPC 2 and Niño-3 SSTs ($r = -0.46$; Fig. 8b) also is not so different when the 1983 episode is removed ($r = -0.36$). The robustness of this mode of streamflow variation also was indicated when the PCA was repeated with 1983 removed from the series. That PCA yielded the same mode with a similar spatial pattern and similar variance capture (8.3%).

Streamflow mode RPC 2 reflects precipitation variations over the same regions. Correlation of this ENSO-related streamflow PC with the gridded precipitation anomalies of Eischeid et al. (1995) indicates that the flow variations correspond to a significant fraction of precipitation variability in South America, with positive precipitation correlations (to this flow RPC) in Amazonia and negative correlations around Paraguay. Furthermore, a PCA of the gridded precipitation anomalies for North and South America yields corresponding precipitation variations as its leading mode (12% of interannual precipitation variance), with the spatial pattern shown in Figure 9. This precipitation pattern (REOF) represents dry El Niños in Central and northernmost South America (through Amazonia) and wet El Niños in southeastern South America and the southern United States (see also the correlations in Fig. 2 of Enfield 1996). Precipitation in northern North America is modestly negatively correlated with SOI in this mode.

Another, less-powerful streamflow mode, RPC 5 (6.5% of interannual streamflow variance), also captures variability related to ENSO (correlation with SOI is $r = 0.44$; Fig. 8c). The associated spatial pattern of flow anomalies, REOF 5 (Fig. 10a), has contrasting streamflow variations in the northwestern and southwestern United States, with streamflow fluctuations along the Chilean coast (roughly from 28°S to 40°S latitude) that are in phase with the southwestern United States (Fig. 10a). The same pattern appears (capturing 7.4% of variance) when the PCA is repeated without 1983, except that the Chilean correlations are muted. Notable extremes of RPC 5 (Fig. 10b) are the strong negative case of 1973 (an El Niño) and strong positive peaks in 1974 and 1976 (two La Niñas). Figures 8c and 10d show that RPC 5 does not depend on the 1983 El Niño (i.e., the 1983 points, with SOI less than -10, correspond to near-zero RPCs in Fig. 8c). Overall, this RPC is associated more with the positive excursions of SOI (La Niñas) than with the negative (Fig. 8c) and is not related to Niño-3 SSTs (Fig. 8d). Correlation of this streamflow mode with the gridded precipitation anomalies of Eischeid et al. (1995) indicated that it corresponds more to precipitation variations in North America (especially in the Pacific Northwest) than elsewhere, but that it captures only a small fraction of precipitation variability even in North America. No single, equivalent precipitation mode was found in the PCA of precipitation anomalies over both Americas.

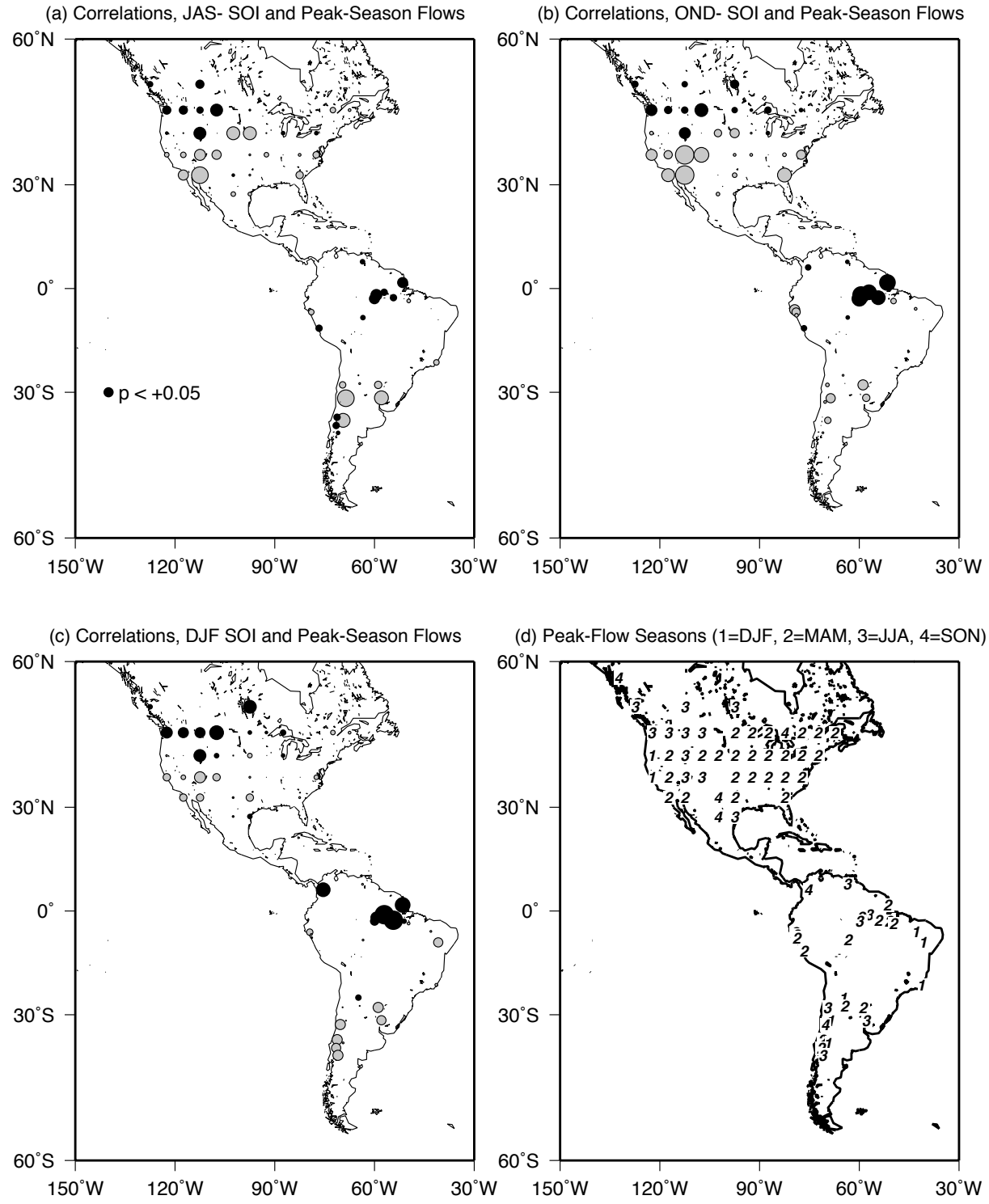

Fig. 5: (a)-(c): Correlations between seasonal Southern Oscillation Index (SOI) averages and peak-season streamflows, 1931-84. Radii of circles are proportional to correlation [radius of minimally significant correlation shown, lower left in panel (a)]; gray circles indicate negative correlations and black circles indicate positive correlations. (d) Seasons of peak flows in average hydrographs. Seasons: DJF, December through February; MAM, March through May; JJA, June through August; SON, September through November; JAS-, July through September of the previous year; OND-, October through December of the previous year.

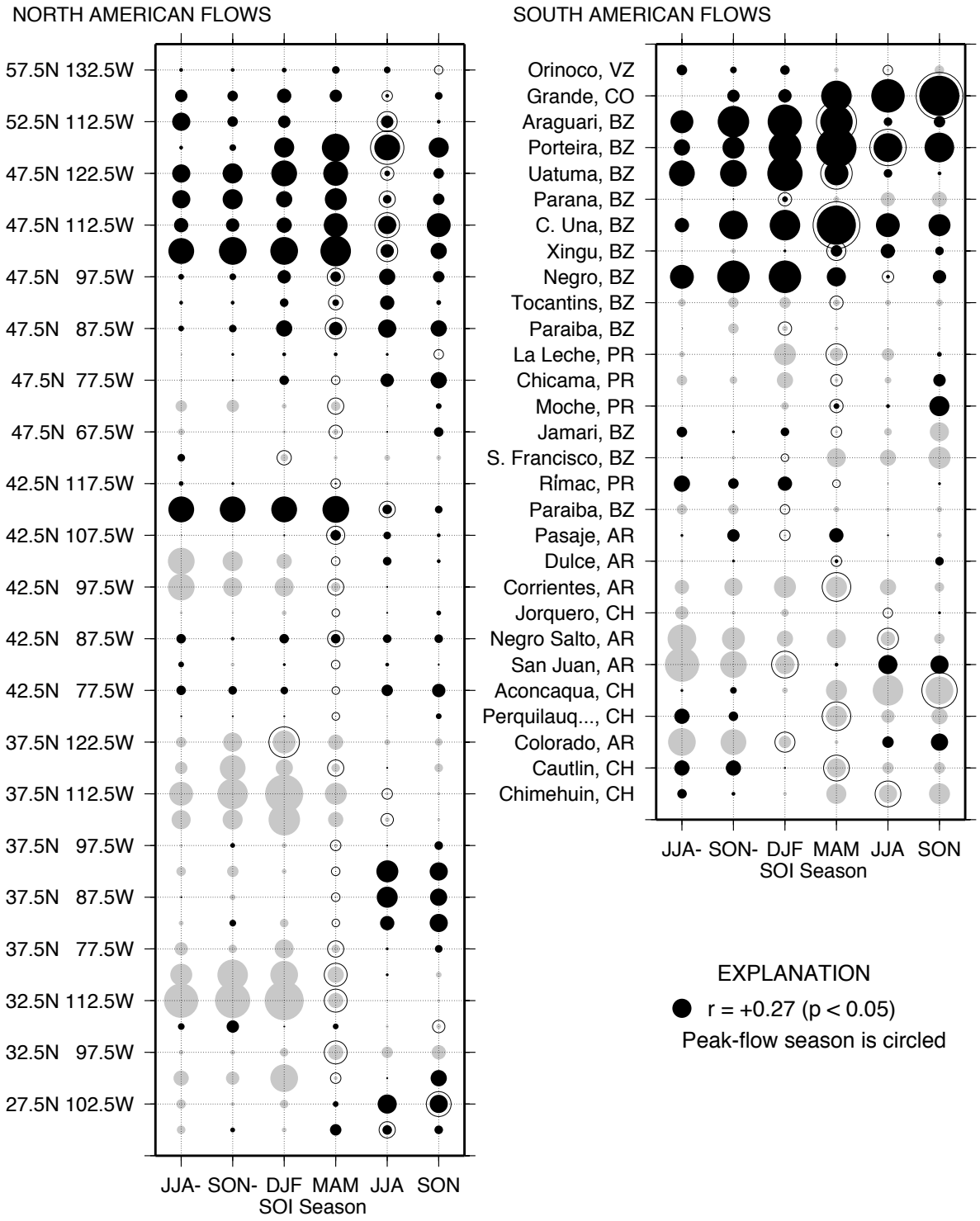

Fig. 6: Correlations between North and South American peak-season flows and seasonal Southern Oscillation Indices, 1931-84. Radii of circles are proportional to correlation (radius of minimally significant correlation shown, lower right); black circles indicate positive correlations, gray circles indicate negative correlations. Sites are sorted from north (top) to south (bottom) in each panel; North American sites are from the gridded series and intermediate sites are at intervening 5°x5° grid points. Seasons: JJA-, June through August of preceding year; SON-, September through November of preceding year; DJF, December through February; MAM, March through May; JJA, June through August; SON, September through November.

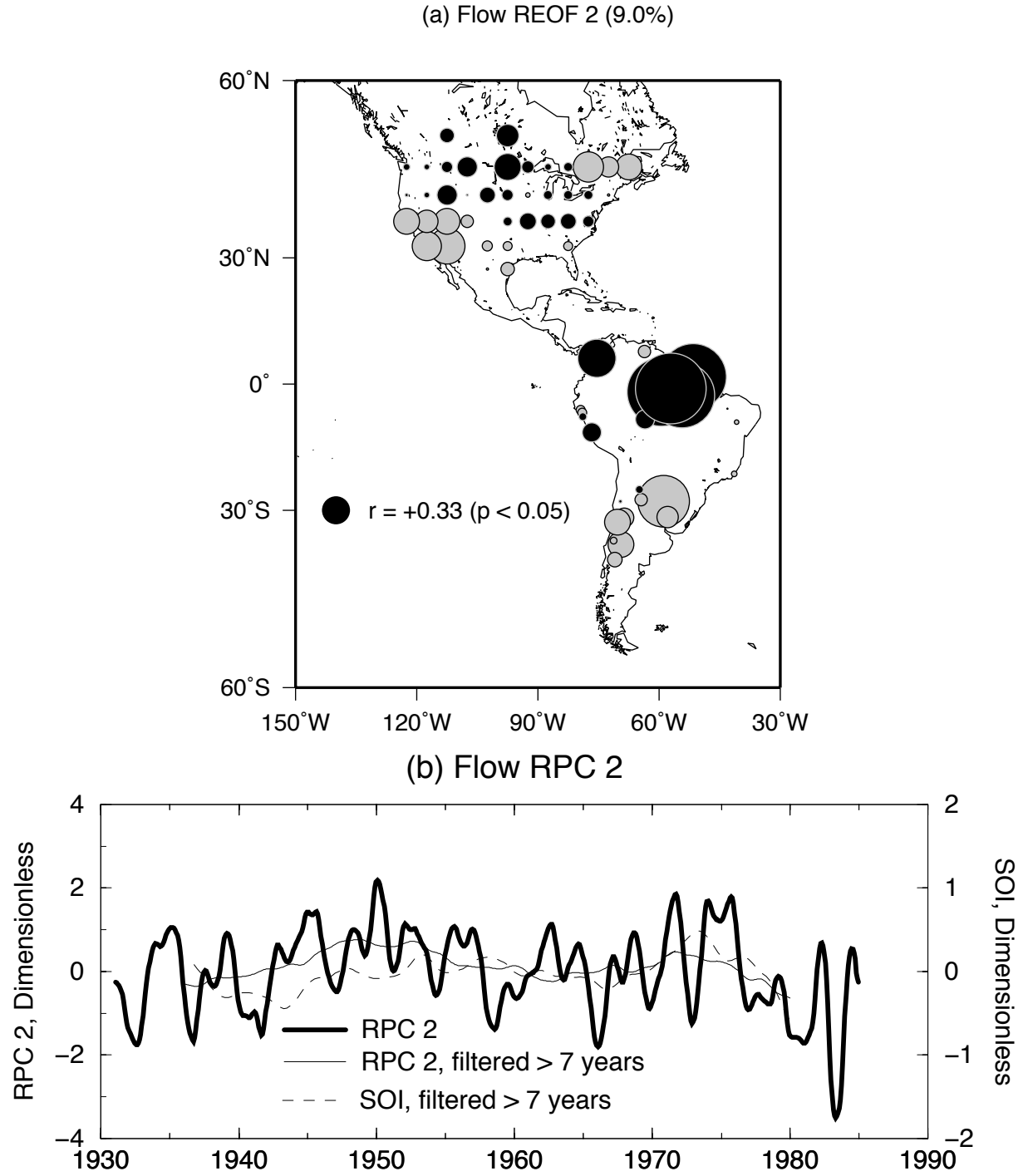

Fig. 7: Second rotated empirical orthogonal function (REOF) and principal component (RPC) of North and South American streamflows, 1931-84: (a) REOF as correlations with the RPC series, black where positive correlations and gray where negative; (b) RPC series (heavy curve), with RPC series (thin solid curve) and Southern Oscillations Index (thin dashed curve) low-pass filtered for variations slower than 7 years. Principal component analysis was performed on flows low-pass filtered with a half-power point at 18 months.

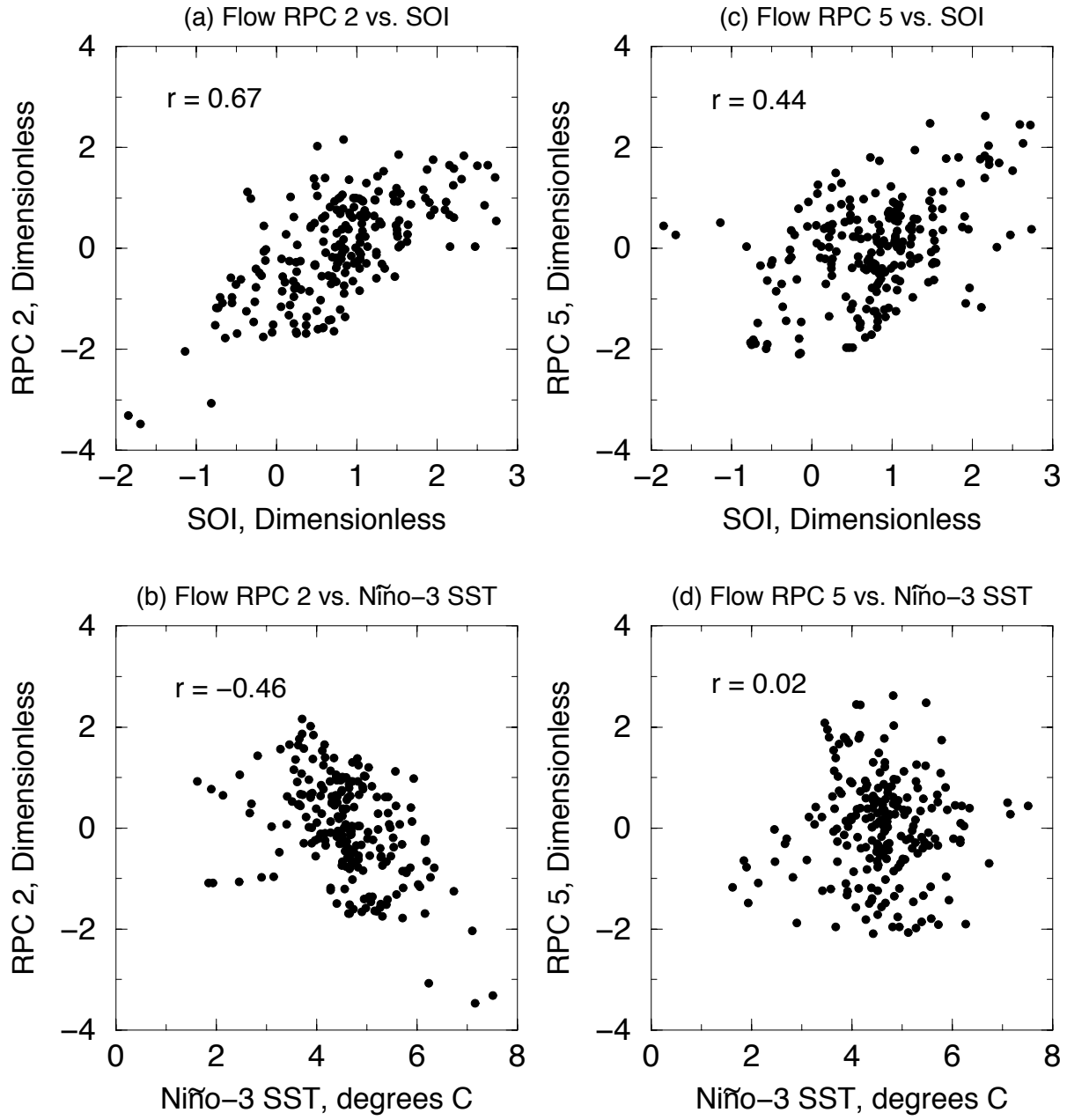

Fig. 8: Rotated principal components (RPCs) and seasonal Southern Oscillation Indices (SOIs) and Niño-3 sea surface temperatures (SSTs): (a) RPC 2 with SOI, (b) RPC 2 with Niño-3 SST, (c) RPC 5 with SOI, and (d) RPC 5 with Niño-3 SSTs.

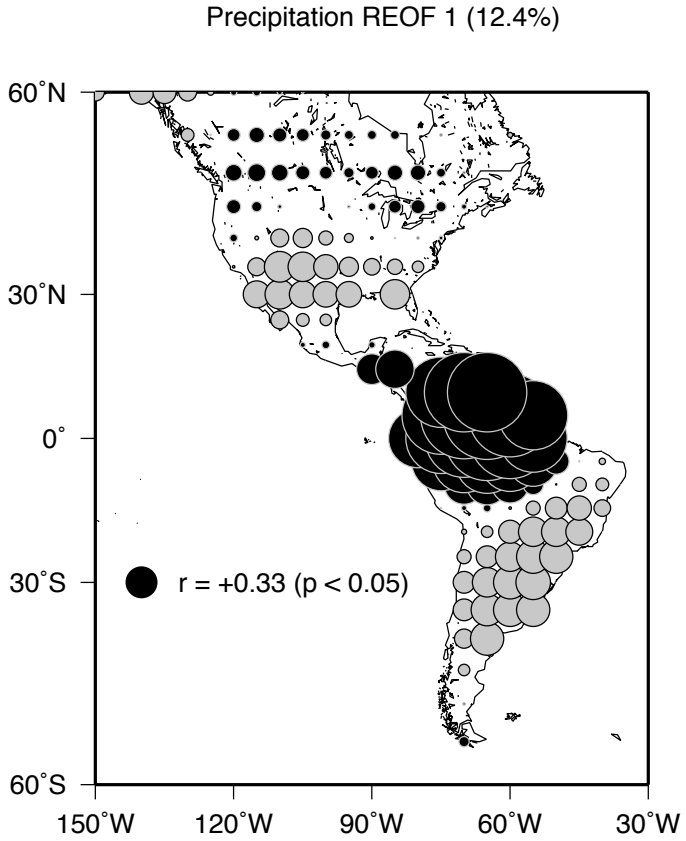

Fig. 9: Same as for Fig. 7a and b, except for the first rotated empirical orthogonal function of North and South American precipitation, 1900-92.

Thus the broad spatial patterns of SOI-streamflow correlation shown in previous sections reflect two principal modes of interannual streamflow variation, one in which the tropical South American streamflow responses to ENSO(excepting Peruvian and, presumably, Ecuadoran rivers) are consistently in the opposite sense from the subtropical streamflow responses, and another in which northern and southern North American streamflow responses are opposites of each other. These flow modes correspond directly to ENSO-driven precipitation variations and constitute about 15% of the overall interannual variance of the (normalized) American streamflows studied here. The two modes differ in their spatial emphases and in when they have been most prominent, but each is reflected in streamflow during several ENSO events. The global climatic conditions associated with the two modes will be discussed more later.

Multiple time-scale aspects of ENSO-streamflow relations

Cayan et al. (1998) have shown that the variance of North American precipitation totals derives almost as much from decadal fluctuations as from interannual variations. Marengo (1995) has found large decadal precipitation and streamflow fluctuations in South America, which can look like trends when records are short. Computation of the percentages of annual streamflow variance that are slower than $(7 \text{ years})^{-1}$ in the present dataset also indicates that, in most of the western Hemisphere, decadal and slower streamflow variations contribute almost as much to year-

to-year variance as do streamflow variations in the frequency range from about (2 years)$^{-1}$ to (7 years)$^{-1}$.

Thus, the multiscale aspects of ENSO-streamflow relations must be considered in order to understand overall streamflow variability. Typically, the ENSO influences in climatic records appear mostly as interannual fluctuations, at least in part because records are short and decadal fluctuations in them are few. However, long-term variations in the character of ENSO are present. During this century, some decades have yielded frequent and vigorous ENSO episodes, whereas others have had relatively weak and infrequent episodes. Most notably, the time intervals from the 1930s through the 1960s had somewhat weaker ENSO variations relative to the first decades of the century and the decades beginning with the 1970s (Fig. 1; see also Rasmusson and Carpenter 1982, Cole et al. 1993). Similarly, during some decades (e.g., 1950s and 1970s), cool tropical episodes (La Niñas, positive SOIs) were more common, whereas during others (e.g., 1980s and 1990s), warm episodes were common. Given these decadal differences in ENSO variability and because streamflow responses to positive and negative SOI conditions, it is natural to wonder if streamflow variations in response to ENSO are similar on all time scales.

Streamflow coherency with SOI

The PCA of Western Hemisphere streamflow variations suggested that two distinct forms of ENSO response may exist, one emphasizing the tropics and the other emphasizing the extratropics. Some of the distinction may be due to the differing multiscale ENSO responses by rivers emphasized by the two RPCs. In particular, streamflows in the tropical rivers tend to follow SOI coherently over all historical time scales whereas extratropical rivers appear to follow SOI in scattered, narrow frequency bands. The close interannual relations between ENSO and the tropical streamflows east of the Andes are suggested by the linear relations between ENSO indices and streamflow RPC 2 in Figure 8a and 8b. Some of the close connection on decadal time scales is evident in Figure 7b, where decadally filtered versions of RPC 2 and SOI can be compared as the two light curves. Examination of streamflow series from individual tropical rivers shows the decadal links to SOI even more clearly; e.g., streamflows in the Araguari River of Brazil correlate with SOI at $r = 0.92$ on decadal time scales.

Extratropical rivers in the Americas are correlated to SOI within much narrower frequency bands. To show in detail how closely the eastern tropical streamflows follow SOI and how different is the extratropical response, coherency spectra of SOI with regional averages of streamflow variations in North and South America are presented in Figure 11. Coherency spectra are essentially correlations squared between two time series, calculated in each of many narrow frequency bands. In Figure 11, only those coherencies that correspond to $p < 0.10$ or better significance levels are shown. Clearly, the thin solid curve for the tropical South American streamflow variations is the only one that is coherent with SOI at all frequencies shown. The other regional streamflow variations are weakly coherent with SOI and, then, only at isolated frequencies. Western and central North American flow modes are coherent with SOI at some interannual frequencies, notably around the quasiquadrennial and quasibiennial ENSO bands (Rasmusson et al. 1990, Jiang et al. 1995). Western North American (Californian) and all four extratropical South American regions are coherent with SOI at decadal and slower frequencies.

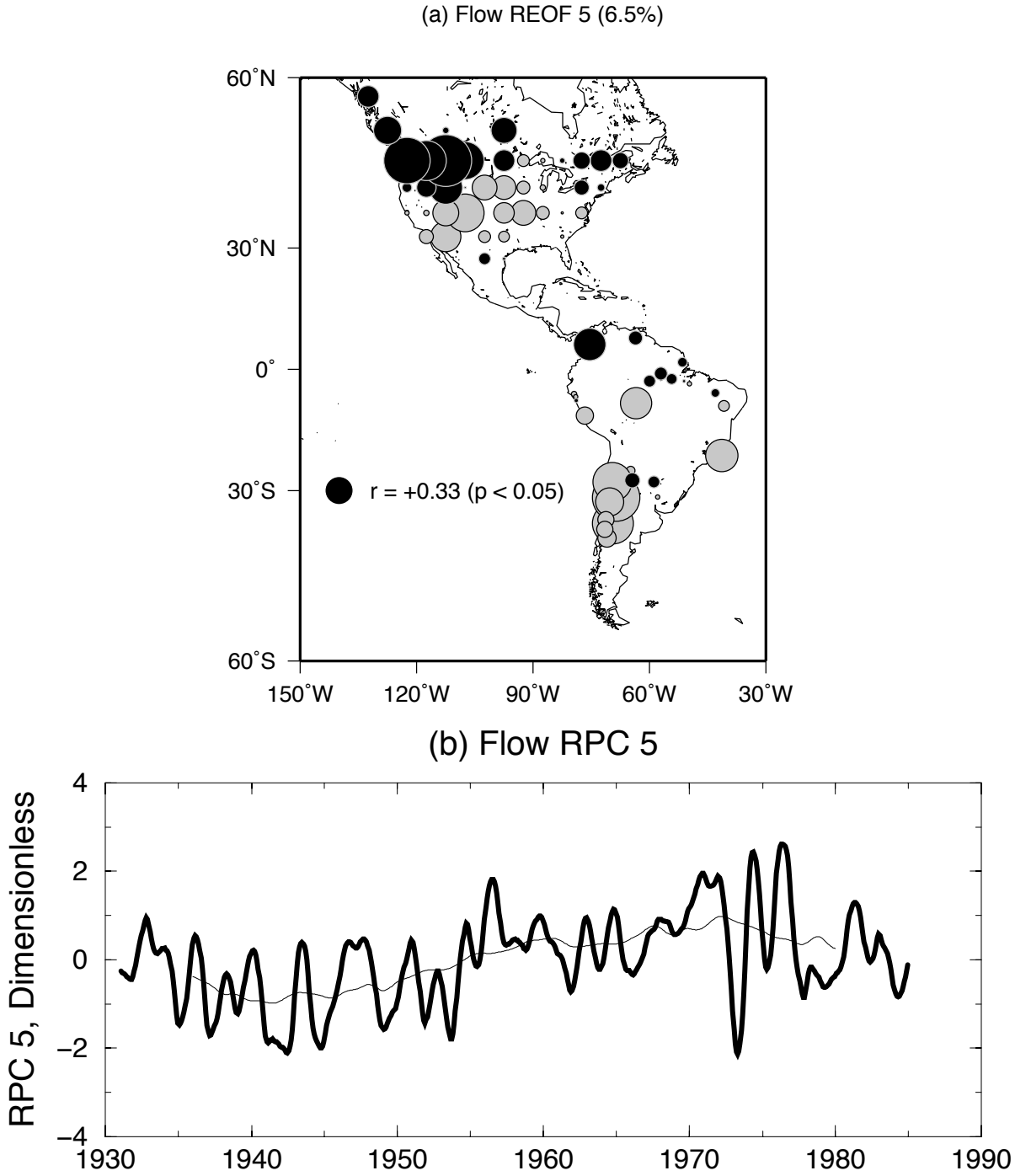

Fig. 10: Same as for Fig.7, except for the fifth rotated empirical orthogonal function and principal component of North and South American streamflows, 1931-84.

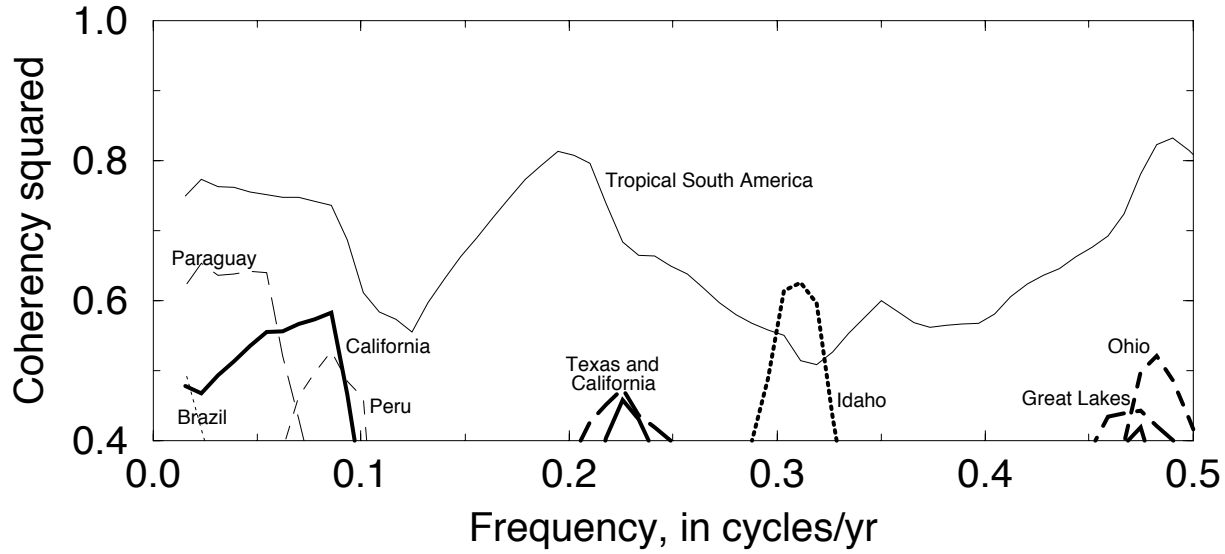

Fig. 11: Coherency squared of regional streamflow variations with respect to Southern Oscillation Index; lower bound marks significance level of roughly $p < 0.1$. 'Tropical South America' refers to rivers east of the Andes.

Streamflow RPC correlations with SSTs

Correlation of the streamflow RPCs identified in preceding sections with the long-term global SST anomalies provides another useful means for determining which temporal variations tend to follow ENSO processes on which time scales. Following the analyses of decadal precipitation by Cayan et al. (1998) and Dettinger et al. (1998), we next correlate filtered versions of global SSTs with similarly filtered versions of the two pan-American flow RPCs associated with ENSO.

The correlations of the streamflow RPC 2 (Fig. 7b) with global SST anomalies are shown in Figure 12 for variations (a) slower than 18 months, (b) between 18 months and 84 months (7 years), and (c) slower than 84 months. Notice that, taken together, the variations analyzed in Figures 12b and 12c make up the variations analyzed in Figure 12a. A dip in the coherencies of Figure 11 near 7 years ($f = 0.14$ cycle/yr) suggests that $(7 \text{ years})^{-1}$ is a reasonable divide between interannual and decadal frequencies. At all three time scales, the SST correlations are dominated by large negative correlations ($r < -0.6$) along the equatorial Pacific and equatorial Indian Ocean and by positive correlations in the central North Pacific ($r > +0.6$) and central South Pacific. In Figures 12a and 12b, correlations greater than about 0.3 or less than about -0.3 are significantly different from zero at $p = 0.05$ levels. The larger correlations in Figure 12c are the result of far fewer realizations of these slow variations during the 1931-84 period. For those decadal variations, the largest correlations in Figure 12c ($|r| \sim 0.8$), however, do reach the level of significance with $p \sim 0.05$.

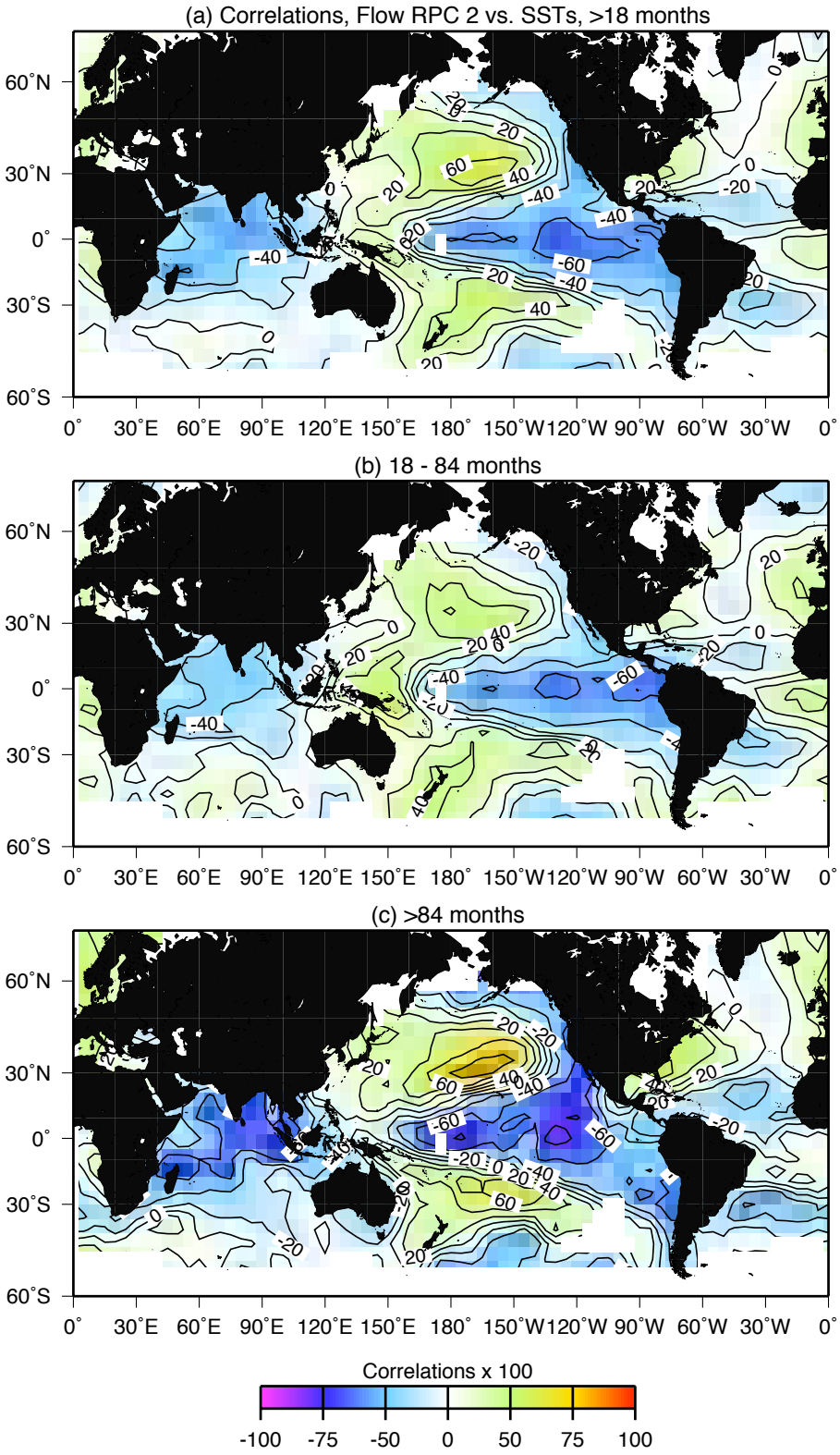

Fig. 12: Correlations (x100) between rotated principal component (RPC) 2 of North and South American streamflows with global sea surface temperature anomalies for variations (a) > 18 months, (b) 18-84 months, and (c) > 84 months (7 years).

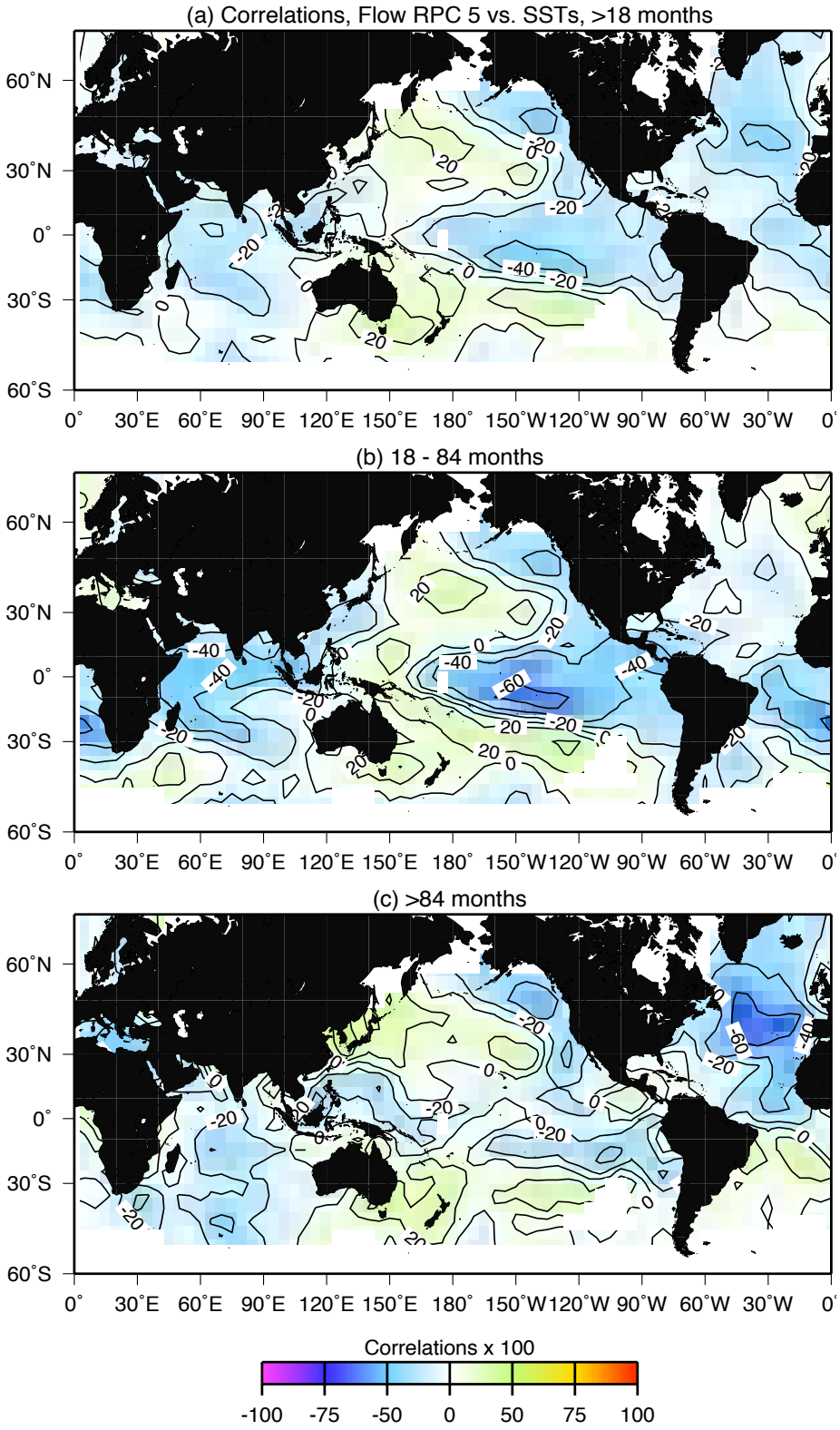

Fig. 13: Same as Fig. 12, except for rotated streamflow principal component (RPC) 5.

Interpreted as signs and strengths of the SST anomalies associated with positive excursions of the streamflow RPC, the pattern that is shared by all panels in Figure 12 is characteristic of well-developed ENSO episodes, with positive RPCs corresponding to cool tropical La Niña episodes and negative RPCs corresponding to El Niño episodes. The pattern, with its broad equatorial Pacific expression reaching essentially to Peru, is like the canonical (Type 1) ENSOs of Fu et al. (1986). Kahya and Dracup (1994) found El Niños of this form to be the most consistently expressed ENSO form in streamflows of the North American Southwest. Variations of this streamflow RPC are significantly associated with ENSO or ENSO-like SST and climate variations on both interannual and decadal time scales, which may indicate that the physical mechanisms that drive both time scales are similar (e.g., Zhang et al. 1997). Correlations (not shown here) between SSTs and the first precipitation RPC (corresponding to the REOF in Fig. 9)--which corresponds to this streamflow mode--also are ENSO-like on all three time scales, although they are less clearly so on the decadal scale. Correlations of this flow mode with similarly filtered SLP anomalies (not shown) yields, on all three time scales, a global Southern Oscillation pattern (a Walker cell with positive correlations radiating northwestward and southeastward from the eastern tropical Pacific region in opposition to negative correlations along the rest of the equator and over much of the rest of the globe; see Allan et al. 1996).

In contrast, streamflow RPC 5 (Fig. 10) is related to ENSO-like variations on interannual time scales, but is associated with a different SST pattern on the decadal time scale. (Fig. 12). The overall correlation pattern (Fig. 13a) is similar in the Pacific and Indian Oceans to the ENSO-like pattern of SST correlations to RPC 2 (Fig. 12a). Similarly, the interannual correlations (Fig. 13b) are dominated by negative correlations in the central equatorial Pacific (the Niño-3 region) with ENSO-like patterns evident in the tropics but weakly expressed in the extratropics (compared to Fig. 12b). The tropical part of this interannual pattern is localized in the central tropical Pacific, more like the Type 2 ENSO of Fu et al. (1986) than was Figure 12b. In contrast, the decadal SST correlations (Fig. 13c) are concentrated in the North Atlantic, which is known to exhibit considerable decadal variability (see Schlosser et al. 1991, Deser and Blackmon 1993, Chen and Ghil 1996). The decadal variations of this RPC (thin line, Fig. 10b) are roughly the opposite of a gradual decline in the North Atlantic Oscillation Index (SLP differences between Iceland and Portugal) from the 1940s to the late 1960s, followed by a recent increase (see Hurrell 1995). Correlations of this flow mode with SLP anomalies (not shown) yield weak correlations in a Southern Oscillation pattern on interannual time scales and a correlation pattern dominated by SLP contrasts between the northern latitudes and the rest of the world, with emphases over North America.

Decadal variations of ENSO teleconnections

Within the time frame for which we have hemispheric streamflow data, the most important multiscale aspect of hydrologic variability associated with ENSO may be a marked change in the patterns of correlations between hydrologic variations and ENSO indices in the early to middle decades of this century. A decided weakening of ENSO processes from about the 1920s through (at least) the 1950s has been noted by several authors (e.g., Troup 1965, Rasmusson and Carpenter 1982, Trenberth 1984, Trenberth and Shea 1987, Elliot and Angell 1988, Lough 1991, 1993, Cole et al. 1993). This weakening has been described in terms of fewer and less-intense warmings, weaker SOI correlations, and changes in the pressure distributions and tropical precipitation.

The multidecadal weakening resulted in a marked change in streamflow relations, or teleconnections, to ENSO. To illustrate this change, the points plotted in Figures 8a and 8c were separated into 1931-55 and 1960-84 subsets and replotted in Figure 14. Most of the correlation between the streamflow RPC 2 and SOI in Figure 8a is shown in Figure 14 to be the result of a relatively strong linear relation between streamflow RPC 2 and SOI during the 1960-84 period with only a slight contribution from the 1931-55 period. Similarly, the more modest correlation between streamflow RPC 5 and SOI in Figure 8c was derived mostly from the recent decades (Fig. 14d) rather than the earlier epoch (Fig. 14c). Similar regional differences are evident when the RPC/Niño-3 SST scatter plots in Figures 8b and 8d are divided into the same epochs.

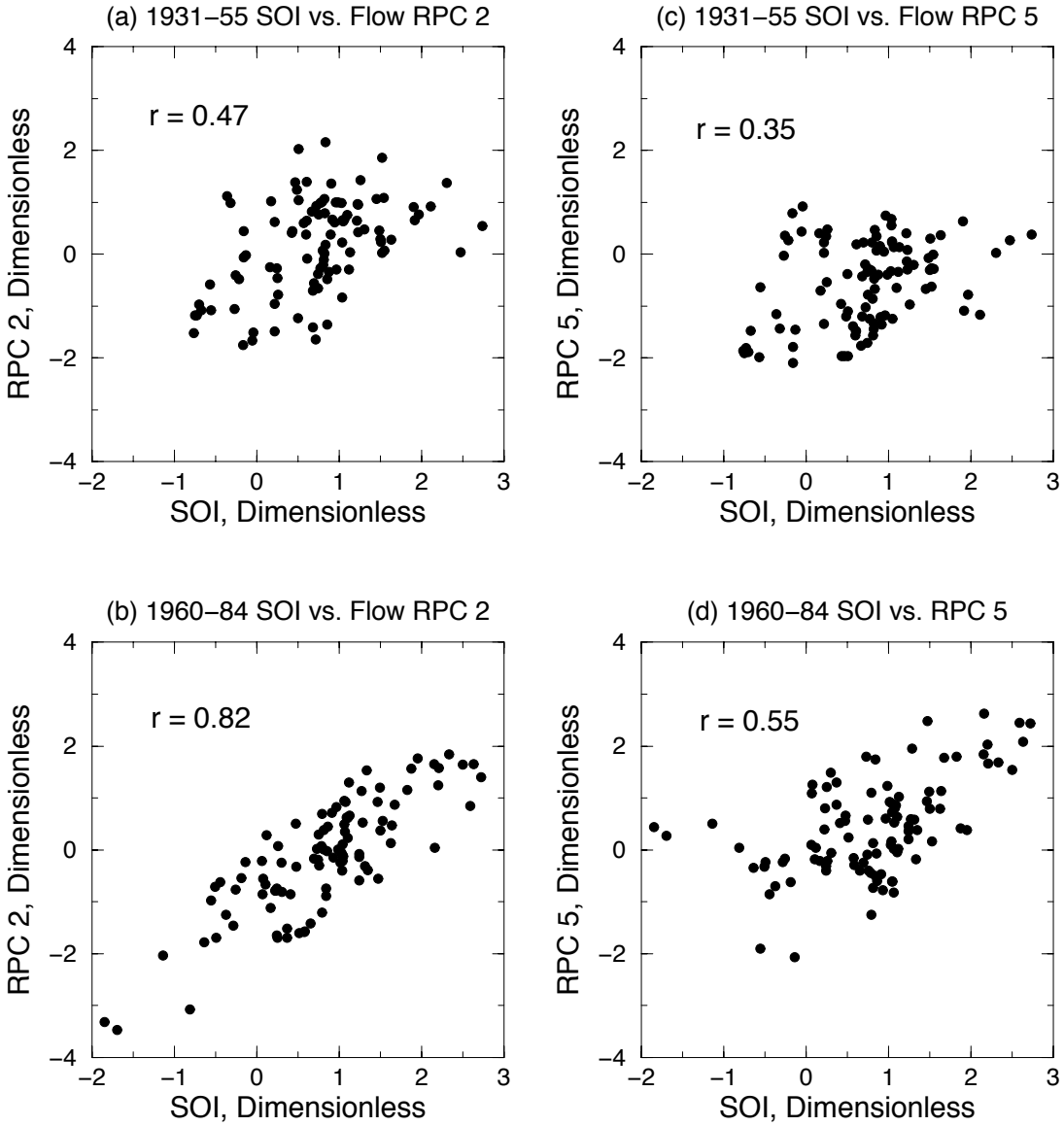

Fig. 14: Same as panels of Fig. 8, except for (a) 1931-55 Southern Oscillation Index (SOI) and flow rotated principal component (RPC) 2, (b) 1960-84 SOI and flow RPC 2, (c) 1931-55 SOI and flow RPC 5, and (d) 1960-84 SOI and flow RPC 5.

The long-term change in ENSO teleconnections early this century also interfered with the close multiscale correlation of tropical streamflows with SOI. Coherency spectra of averaged tropical streamflows (light solid curve, Fig. 11) during the time intervals 1931-55, 1960-84, and 1931-84 are shown in Figure 15a. Window widths were adjusted so that significance levels are similar from curve to curve. Clearly, coherencies at most frequencies--except around $(4\ \text{year})^{-1}$ to $(6\text{-year})^{-1}$, in the lower interannual ENSO frequencies of Rasmusson et al. (1990) and Jiang et al. (1995)--have been much larger in recent decades (light solid curve, Fig. 15a) than in previous ones (dashed curve, Fig. 15a). In the Araguari River in Amazonia, this change in coherency was reflected in an abrupt change in 21-year correlations between annual flows and SOI from roughly +0.1 (and not significantly different from zero) prior to 1960 to about +0.75 in the 1970s and 1980s (Fig. 15b). For other regions, which were shown in Figure 11 to be coherent with SOI in narrow frequency bands, the coherency spectra (not shown) generally increase from the 1931-55 to 1960-84 time intervals, with particularly widespread coherency gains in the lower ENSO frequency band. Correlations between many streamflow and precipitation series outside the tropics and SOI (or other tropical ENSO indices) show decadal changes similar to those found in the tropical rivers; e.g., 21-year correlations between Arizona precipitation and the preceding summer's Niño-3 SSTs shown in Figure 15b illustrate the extratropical hydrologic changes.

These changes may be associated partly with changes in the quality and representativeness of the SOI series during early parts of the century (Trenberth 1984, Trenberth and Shea 1987), but, in large part, they appear to reflect actual changes in the hemispheric influence of ENSO. As was mentioned above, Niño-3 SSTs can be substituted for SOI in Figure 14 with similar disparity of correlations from earlier decades to recent decades.

Reasons for the reduced hydrologic/ENSO teleconnections during the 1930s to 1950s period are uncertain. The change in expressions of the ENSO phenomenon in the tropics has been ascribed to the weakening of the ENSO process during that earlier period, and comparison of the 21-year standard deviations of SOI with the corresponding correlations between SOI and Niño-3 SSTs, shown by solid circles in Figure 16, indicates that the oceanic (Niño-3 SST) and atmospheric (SOI) expressions of ENSO *did* become disconnected during decades when one or the other is weak (and usually when both are weak, because the 21-year standard deviations of SOI and Niño-3 are correlated with $r = +0.83$). A similar plot of SOI standard deviations versus correlations of SOI and Arizona precipitation (open circles in Fig. 16) shows that, when SOI variability is low (on decadal time scales), this (and essentially all other tropical and North American) hydrologic teleconnection weakens to the point of failing. Regionally, correlations of SOI with the streamflow RPCs decline along with the standard deviation of SOI, in 21-year windows like those used in Fig. 16. On interannual time scales, Enfield and Luis Cid (1991) have suggested that one form of hydrologic response arises when SOI (and ENSO) is strongly positive or negative, and another when ENSO variation is weak. Kumar and Hoerling (1997) observed this kind of response in simulated responses to ENSO-like forcings.

Overall, streamflow RPC 2 was well correlated with ENSO on both interannual and decadal timescales whereas RPC 5 was correlated to ENSO only on the interannual timescale. These different styles of ENSO response, together with evidence of decadally varying ENSO teleconnections, suggested that separate PCAs for the two epochs might uncover different streamflow-response patterns. Interestingly, however, the changes in hydrologic teleconnections as ENSO weakened on decadal time scales from about the 1920s into the 1950s had a relatively limited influence on the PCA patterns obtained from North and South American streamflows. When the PCA was repeated, but with only the time series from 1931-55, streamflow RPCs with

spatial patterns quite similar to the original RPC 2 and RPC 5 modes were obtained and captured 9.9% and 9.3% of variance, respectively. Principal component analysis of streamflows from 1960-84 reveals a recent ENSO flow mode with a spatial pattern that appears to be a sum of the original RPC 2 and RPC 5 (including cancellation of the contrasting streamflow correlations in eastern North America in Figs. 7 and 10).

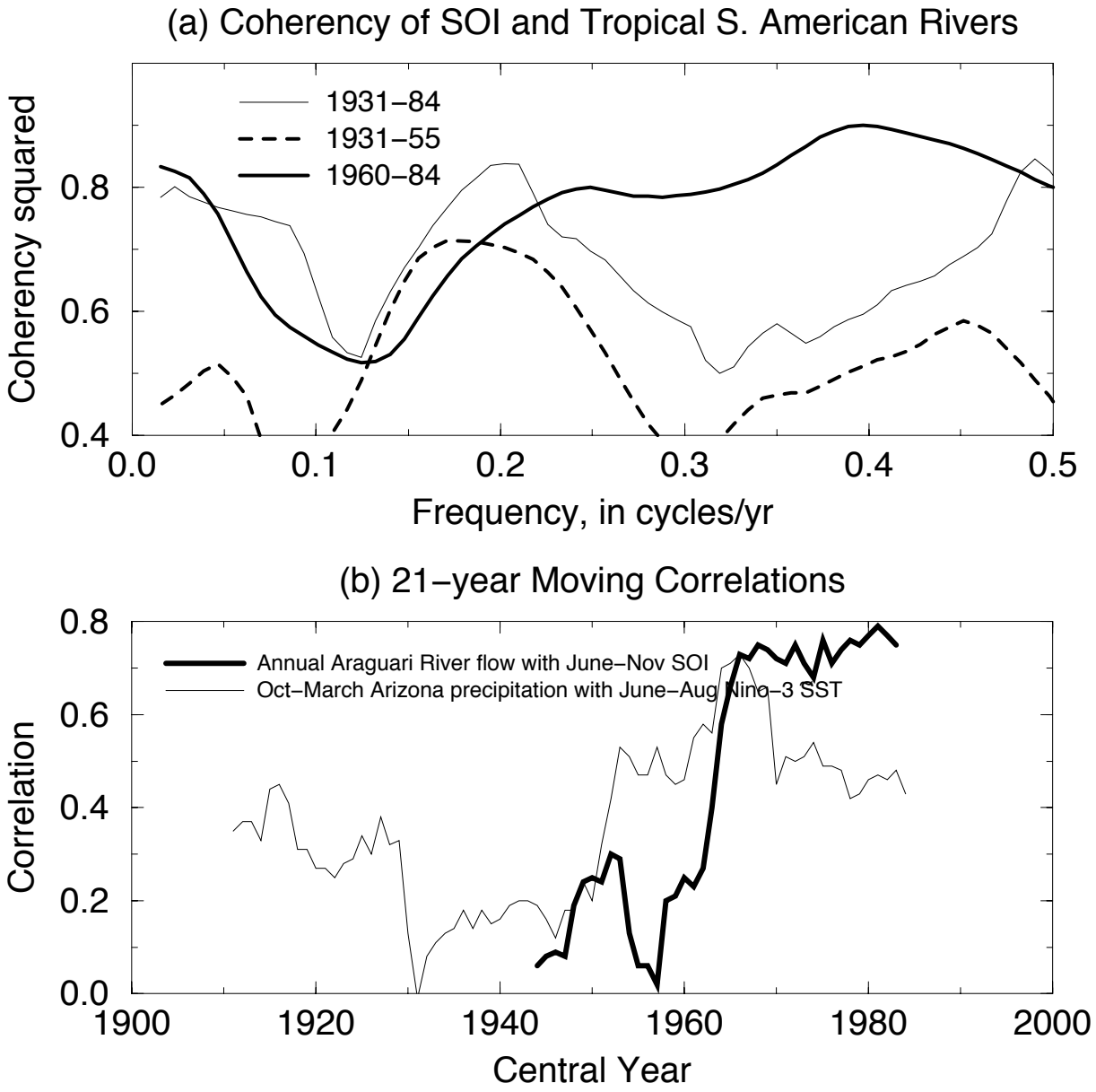

Fig. 15: Coherency squared of tropical South American streamflow variations (east of the Andes) with respect to Southern Oscillation Index (SOI) during several different epochs; lower bound marks significance level of roughly $p < 0.1$; (b) 21-year moving correlations of annual Araguari River flows with June-November SOI, and of October-March Arizona precipitation with June-August Niño-3 sea surface temperatures; correlations greater than 0.4 are significantly different from zero at $p<0.05$.

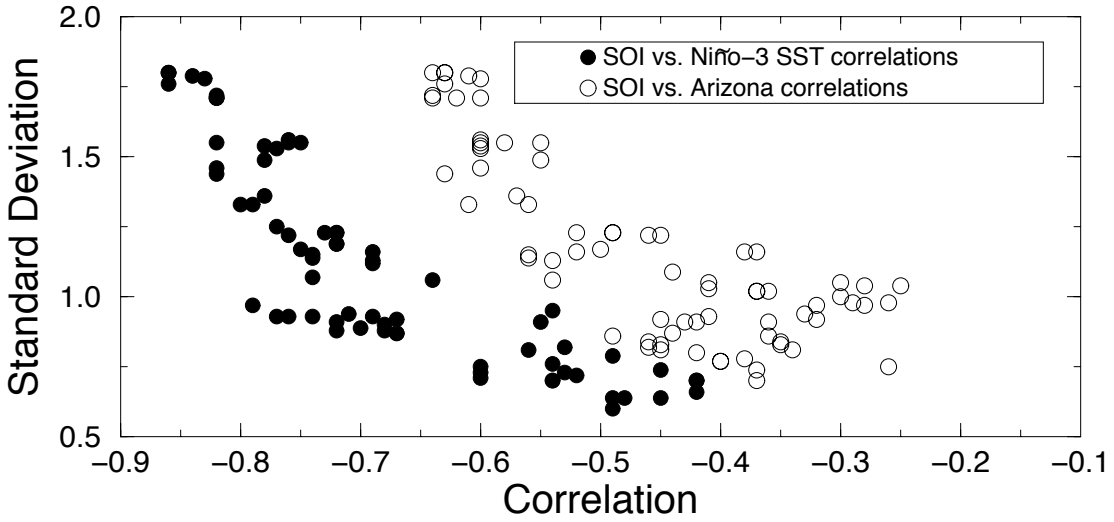

Fig. 16: Comparisons of the correlation coefficients (solid circles) of October through December (OND) Southern Oscillation Index (SOI) and Niño3 sea surface temperatures (in 20-year windows) with OND SOI standard deviations in the same 20-year windows, 1931-90; and the correlation coefficients (open circles) of OND SOI and Arizona-5 climate division October-March precipitation (in 20-year windows) with OND SOI standard deviations in the same 20-year windows, 1931-90.

The consolidation of ENSO-related flow PC patterns in the recent subset of American flows suggests that the two RPCs in the original analysis may have been a way for (inherently linear) PCA to capture a nonlinear or nonstationary ENSO relationship in which strong ENSOs, decades with strong ENSO variability, or decades with strong ENSO teleconnections elicit patterns of streamflow response that are different from those of weak ENSOs. Alternatively, the two streamflow RPCs, with their different spatial patterns, may be a PCA response to asymmetries in El Niño and La Niña flow patterns (Hoerling et al. 1997), a PCA response to ENSO-response patterns that are sometimes modified by subtle inter-ENSO differences or extratropical influences, or even statistical artifacts (e.g., Newman and Sardeshmukh 1995). In any case, the different styles of streamflow response to multiscale ENSO variability in the tropics and extratropics provides reason enough to believe that at least two modes of ENSO-streamflow response exist.

Conclusions

Anticipation of year-to-year streamflow variations has a vital role in long-term management of water supplies and hazards nearly everywhere, and an understanding of the physical and statistical connections between streamflow variations and El Niño/Southern Oscillation (ENSO) processes provides a useful starting point. ENSO processes are more predictable at seasonal and annual time scales than any other year-to-year climate variation, and streamflow responses to ENSO processes are detectable in rivers in many regions of the Earth. In response to tropical and extratropical changes in precipitation and, to a lesser extent, temperatures during the course of warm-tropical El Niño and cool-tropical La Niña episodes, streamflows vary throughout the Americas and Australia, in northern Europe, and in parts of Africa and Asia. Changes in runoff rates between the warm and cool episodes range up to 500 mm/yr and, in relative terms, “amplify” the year-to-year precipitation variations that force them. Changes in runoff from

tropical river basins are nearly all towards less flow during El Niño episodes, with an El Niño average of 15% to 34% less than normal (compared to changes in tropical precipitation of about 9% less than normal in the same areas). Changes in extratropical runoff depend greatly on location and average closer to zero overall. The global responses to El Niños and La Niñas are roughly mirror images of each other, but with differences that may prove important either event by event or on decadal time scales. In North and South America, the relations between the seasonal Southern Oscillation Index (SOI) and peak-flow season streamflows show considerable persistence. In tropical South America east of the Andes, correlations between flows in other seasons with December through February (DJF) SOIs also are notably persistent, whereas, in the extratropical Americas, correlations are smaller when other, non-peak seasons are considered.

At least two styles of streamflow response to ENSO are present in the Western Hemisphere. When interannual North and South American streamflow variations are analyzed together, roughly 6 degrees of freedom can be isolated in the form of principal components but, upon Varimax rotation, only two are found to be associated with ENSO variability. Together these two modes capture about 15% of overall interannual streamflow variability. The more powerful of these modes corresponds mostly to ENSO responses by the rivers of tropical South America east of the Andes, along with streamflow variations in southern South America and the southwestern United States. In this mode, El Niños result in less runoff in Brazil and more runoff in the other regions. The mode is correlated to ENSO-like sea-surface temperature (SST) variations on both interannual and interdecadal time scales. This multiscale SST correlation may reflect similarities in the physical mechanisms that drive this dominant streamflow variation on the two time scales. Notably, the tropical streamflows are coherent with SOI at essentially all historical time scales. This mode of streamflow variation reflects the leading rotated principal component (RPC) of precipitation anomalies over North and South America.

Although the first streamflow component is reflected in many extratropical rivers, a second ENSO-related streamflow mode characterizes another set of extratropical streamflow variations. This second principal component emphasizes the north-south differences in streamflows in North America during El Niños and La Niñas and (less robustly) streamflow variations along the central Andes. This mode is emphasized during La Niñas, and yields wet La Niñas in northwestern North America and dry La Niñas in the Southwest. The relation of this streamflow mode to ENSO seems to be mostly on interannual time scales, with decadal variations in this streamflow pattern following slow fluctuations of North Atlantic SSTs and climate. The extratropical streamflow variations are coherent with SOI variations only within scattered interannual and decadal time scales.

Perhaps the most remarkable decadal variation identified in the ENSO-streamflow relations is the decades-long changes in teleconnections when recent decades are compared to the period from about the 1920s into the 1950s (see also McCabe and Dettinger, in review). During the earlier epoch, large changes in the teleconnections of ENSO to tropical and extratropical streamflows are found, often amounting to near disappearances of those connections. These changes are found in streamflow connections with SOI, Niño-3 SSTs, and even global SST anomalies, and can be detected in the spatial, temporal, and frequency domains. The changes appear to be associated with, at least, a weakening of ENSO variability and the expected interaction of the atmospheric and oceanic components of ENSO during the earlier period (Fig. 16a; see Trenberth and Shea 1987).

The two ENSO-related principal components of North and South American streamflow may reflect part of these long-term changes in ENSO teleconnections; alternatively, they may be

associated with nonlinearities and asymmetries between the warm- versus cool-episode streamflow responses. Overall, responses of streamflow to ENSO variations are widespread, strong, and regular enough to warrant much attention and high hopes for large improvements in hydrologic prediction on interannual time scales. The interplay between streamflow variations and ENSO processes, however, varies from region to region, decade to decade, and even event to event in ways that are significant enough to require careful analysis and caution from forecasters and resource managers. The decadal changes in teleconnections earlier in the twentieth century need to be recognized in interpretations of, and planning for, ENSO-hydrologic connections.

Acknowledgments.

Comments from Drs. C. Perry, U.S. Geological Survey (USGS), Brant Liebmann, National Oceanic and Atmospheric Administration's (NOAA's) Climate Diagnostics Center (CDC), and Henry Diaz, CDC, improved this chapter. Streamflow data used in this chapter came from a number of sources, including: the World Meteorological Organization streamflow archive (courtesy of Roy Jenne, National Center for Atmospheric Research); the USGS Hydroclimatic Data Network (Slack and Landwehr 1992); the National Aeronautic and Space Administration Goddard Distributed Active Archive Center; University of California, Los Angeles, Center for Study of Hydroclimatology in the Pacific Rim; National Climatic Data Center (P. Groisman); New Zealand National Institute for Water and Atmospheric Research and Electricity Corporation of New Zealand (A. McKerchar); Instituto Nacional de Recursos Naturales in Peru; National Weather Service Nile Forecast System; Evaluacion de Recursos, S.A., in Argentina; Southern Africa Development Community in Zambia (C.B. Mwasile); and other contributors. About 20 of the series are not in public domain and come from the Global Runoff Data Center or from Eletrobras and Eletronorte, Brazil. MD's and DC's participation in this study was supported by NOAA Paleoclimatology Program Grant NA56GPO404 and the USGS Global Change Hydrology Program. MD benefited from his extended visit to the NOAA Climate Diagnostics Center, Boulder, Colorado, while preparing this chapter; that visit was made possible by Henry Diaz.

References

Allan, R., Lindesay, J., and Parker, D., 1996: *El Niño, Southern Oscillation and Climate Variability*. Collingwood, Australia: CSIRO Publishing, 405 pp.

Barnett, T. P., Brennecke, K., Limm, J., and Tubbs, A. M., 1984: Construction of a near-global sea-level pressure field. *Scripps Institution of Oceanography Reference Series* 84-7, La Jolla, CA.

Barnett, T. P., Del Genio, A. D., and Ruedy, R. A., 1992: Unforced decadal fluctuations in a coupled model of the atmosphere and ocean mixed layer. *Journal of Geophysical Research*, **97**, 7341- 7354.

Barnston, A. G., and Livezey, R. E., 1987: Classification, seasonality, and persistence of low-frequency atmospheric circulation patterns. *Monthly Weather Review*, **115**, 1083-1126.

Benjamin, J. R., and Cornell, C. A., 1970: *Probability, statistics, and decision for civil engineers*. New York: McGraw-Hill Book Company, 684 pp.

Cayan, D. R., and Webb, R. H., 1992: El Niño/Southern Oscillation and streamflow in the western United States. *In* H.F. Diaz and V. Markgraf (eds.), *El Niño--Historical and Paleoclimatic Aspects of the Southern Oscillation*. Cambridge: Cambridge University Press, 29-68.

Cayan, D. R., Dettinger, M. D., Diaz, H. F., and Graham, N., 1998: Decadal variability of precipitation over western North America. *Journal of Climate*, in press.

Chen, F., and Ghil, M., 1996: Interdecadal variability in a hybrid coupled ocean-atmosphere model. *Journal of Physical Oceanography*, **26**, 1561-1578.

Chiew, F. H. S., McMahon, T. A., Dracup, J., and Piechota, T., 1994: El-Niño/Southern Oscillation and streamflow patterns in South-East Australia. *Transactions, Institution of Engineers, Australia*, **36**, 285-291.

Cole, J. E., Fairbanks, R. G., and Shen, G. T., 1993: Recent variability in the Southern Oscillation: Isotopic results from a Tarawa atoll coral. *Science*, **260**, 1790-1793.

Depetris, P. J., and Kempe, S., 1990: The impact of the El Niño 1982 event on the Parana River, its discharge and carbon transport. *Global and Planetary Change*, **3**, 239-244.

Deser, C., and Blackmon, M., 1993: Surface climate variations over the North Atlantic Ocean during winter: 1900-1989. *Journal of Climate*, **6**, 1743-1753.

Dettinger, M. D., and Cayan, D. R., 1998: Historical modes of interannual and decadal hydroclimatic-hydrologic variability in the Western Hemisphere (abs.). *Pole-Equator-Pole Paleoclimate Workshop*, Merida, Venezuela, March 1998.

Dettinger, M. D., Cayan, D. R., Diaz, H. F., and Meko, D., 1998: North-south precipitation patterns in western North America on interannual-to-decadal time scales. *Journal of Climate*, in press.

Dhar, O. N., and Nandargi, S., 1995: Monsoon activity and flows in Central Indian rivers. *Indian Journal of Power and River Valley Development*:, **45**, 80-90.

Diaz, A. F., Studzinski, C. D., and Mechoso, C. R., 1998: Relationships between precipitation anomalies in Uruguay and southern Brazil and sea surface temperatures in the Pacific and Atlantic Oceans. *Journal of Climate*, **11**, 251-271.

Diaz, H. F., and Kiladis, G. N., 1992: Atmospheric teleconnections associated with the extreme phases of the Southern Oscillation. *In* Diaz, H. F., and Markgraf, V. (eds.), *El Niño--Historical and Paleoclimatic Aspects of the Southern Oscillation*. Cambridge: Cambridge University Press, 7-28.

Douglas, A. V., Cayan, D. R., and Namias, J., 1982: Large-scale changes in North Pacific and North American weather patterns in recent decades. *Monthly Weather Review*, **110**, 1851-1862.

Eischeid, J. K., Baker, C. B., Karl, T. R., and Diaz, H. F., 1995: The quality control of long-term climatological data using objective data analysis. *Journal of Applied Meteorology*, **34**, 2787-2795.

Elliot, W. P., and Angell, J. K., 1988: Evidence for changes in Southern Oscillation relationships during the last 100 years. *Journal of Climate*, **1**, 729-737.

Eltahir, E. A. B., 1996: El Niño and the natural variability in the flow of the Nile River. *Water Resources Research*, **32**, 131-137.

Enfield, D. B., 1996: Relationships of inter-American rainfall to tropical Atlantic and Pacific SST variability. *Geophysical Research Letters*, **23**, 3305-3308.

Enfield, D. B., and Luis Cid, S., 1991: Low frequency changes in El Niño-Southern Oscillation. *Journal of Climate*, **4**, 1137-1146.

Fu, C., Diaz, H. F., and Fletcher, J. O., 1986: Characteristics of the response of sea surface temperature in the central Pacific associated with warm episodes of the Southern Oscillation. *Monthly Weather Review*, **114**, 1716-1738.

Graham, N. E., 1994: Decadal-scale climate variability in the 1970s and 1980s: Observations and model results. *Climate Dynamics*, **10**, 135-162.

Graham, N. E., Barnett, T. P., Wilde, R., Ponater, M., and Schubert, S., 1994: On the roles of tropical and midlatitude SSTs in forcing interannual to interdecadal variability in the winter Northern Hemisphere circulation. *Journal of Climate*, **7**, 1416-1441.

Guetter, A. K., and Georgakakos, K. P., 1996: Are the El Niño and La Niña predictors of the Iowa River seasonal flow? *Journal of Applied Meteorology*, **35**, 690-705.

Hoerling, M. P., Kumar, A., and Zhong, M., 1997: El Niño, La Niña, and the nonlinearity of their teleconnections. *Journal of Climate*, **10**, 1769-1786.

Houghton, R. W., 1996: Subsurface quasi-decadal fluctuations in the North Atlantic. *Journal of Climate*, **9**, 1363-1373.

Hurrell, J. W., 1995: Decadal trends in the North Atlantic Oscillation: Regional temperatures and precipitation. *Science*, **269**, 676-679.

Jacobs, G. A., Hurlbert, J. C., Kindle, J. C., Metzger, E. J., Mitchell, J. L., Teague, W. J., and Wallcraft, A. J., 1994: Decade-scale trans-Pacific propagation and warming effects of an El Niño anomaly. *Nature*, **370**, 360-363.

Jiang, N., Neelin, J. D., and Ghil, M., 1995: Quasi-quadrennial and quasi-biennial variability in the equatorial Pacific. *Climate Dynamics*, **12**, 101-112.

Kahya, E., and Dracup, J. A., 1993: U.S. Streamflow patterns in relation to the El Niño/Southern Oscillation. *Water Resources Research*, **29**, 2491- 2503.

Kahya, E., and Dracup, J. A., 1994: The influences of type 1 El Niño and La Niña events on streamflows in the Pacific Southwest of the United States. *Journal of Climate*, **7**, 965-976.

Kaylor, R. E., 1977: *Filtering and Decimation of Digital Time Series*. College Park: Institute of Physical Science and Technology, University of Maryland, Technical Report BN850, 14 pp.

Kazadi, S. N., 1996: Interannual and long-term climate variability over the Zaire River basin during the last 30 years. *Journal of Geophysical Research*, **101**, 21351-21360.

Kiladis, G. N., and Diaz, H. F., 1989: Global climatic anomalies associated with extremes of the Southern Oscillation. *Journal of Climate*, **2**, 1029-1090.

Koch, R. W., Buzzard, C. F., and Johnson, D. M., 1991: Variation of snow water equivalent and streamflow in relation to the El Niño/ Southern Oscillation. *Proceedings*, *Western Snow Conference*, **59**, 37.

Kumar, A., and Hoerling, M. P., 1997: Interpretation and implications of the observed inter-El Niño variability. *Journal of Climate*, **10**, 83-91.

Latif, M., and Barnett, T. P., 1994: Causes of decadal climate variability over the North Pacific and North America. *Science*, **266**, 634-637.

Lettenmaier, D. P., Wood, E. F., and Wallis, J. R., 1994: Hydro-climatological trends in the continental United States, 1948-88. *Journal of Climate*, **7**, 586-607.

Lins, H. F., 1985a: Streamflow variability in the United States: 1931-78. *Journal of Climate and Applied Meteorology*, **24**, 463-471.

Lins, H. F., 1985b: Interannual streamflow variability in the United States based on principal components. *Water Resources Research,* **21**, 691-701.

Lough, J. M., 1991: Rainfall variations in Queensland, Australia: 1891-1986. *International Journal of Climatology*, **11**, 745-768.

Lough, J. M., 1993: Variations of some seasonal rainfall characteristics in Queensland, Australia: 1921-1987. *International Journal of Climatology*, **13**, 391-409.

Manly, B.F.J., 1986: *Multivariate statistical methods*. London, Chapman and Hall, 159 p.

Marengo, J., 1995: Variations and change in South American streamflow. *Climatic Change*, **31**, 99-117.

Marengo, J. A., Tomsella, J., and Uvo, C. R., 1998: Long-term streamflow and rainfall fluctuations in tropical South America: Amazonia, East Brazil, and Northwest Peru. *Journal of Geophysical Research,* **103**, 1775-1783.

McCabe, G. J., and Dettinger, M. D., in review: Decadal variability in the strength of ENSO teleconnections with precipitation in the Western United States. *Journal of Cimate*.

Moss, M. E., Pearson, C. P., and McKerchar, A. I., 1994: The Southern Oscillation index as a predictor of the probability of low streamflows in New Zealand. *Water Resources Research,* **30**, 2717-2723.

Newman, M., and Sardeshmukh, P. D., 1995: A caveat concerning Singular Value Decomposition. *Journal of Climate*, **8**, 353-360.

Nichollis, N., 1992: Historical El Niño/Southern Oscillation variability in the Australasian region. *In* Diaz, H. F., and Markgraf, V. (eds.), *El Niño--Historical and Paleoclimatic Aspects of the Southern Oscillation*. Cambridge: Cambridge University Press, 151-173.

North, G. E., Bell, T. L., Cahalan, R. F., and Moeng, F. J., 1982: Sampling errors in the estimation of empirical orthogonal functions. *Monthly Weather Review*, **110**, 699-702.

Parker, D. E., Folland, C. K., Bevan, A., Ward, M. N., Jackson, M., and Maskell, K., 1995: Marine surface data for analysis of climatic fluctuations on interannual to century timescales. *In* Martinson, D. G., et al. (eds.), *Natural Climate Variability on Decade-to-Century Time Scales*. Washington: National Academy Press, 241-250.

Piechota, T. C., and Dracup, J. A., 1996: Drought and regional hydrologic variation in the United States: Associations with the El Niño-Southern Oscillation.*Water Resources Research*, **32**, 1359-1374.

Pisciottano, G., Diaz, A., and Mechoso, C. R., 1994: El Niño-Southern Oscillation Impact on Rainfall in Uruguay. *Journal of Climate*, **7**, 1286-1303.

Probst, J. L., and Tardy, Y., 1987: Long range streamflow and world continental runoff fluctuations since the beginning of this century. *Journal of Hydrology*, **94**, 289-311.

Probst, J. L., and Tardy, Y., 1989: Global runoff fluctuations during the last 80 years in relation to world temperature change. *American Journal of Science*, **289**, 267-285.

Quinn, W. H., 1992: A study of Southern Oscillation-related climatic activity for A.D. 622-1900 incorporating Nile River flood data. *In* Diaz, H.F., and Markgraf, V. (eds.), *El Niño--Historical and Paleoclimatic Aspects of the Southern Oscillation*. Cambridge: Cambridge University Press,119-149.

Rao, V. B., and Hada, K., 1990: Characteristics of rainfall over Brazil: Annual variations and connections with the Southern Oscillation. *Theoretical and Applied Climatology*, **42**, 81-91.

Rasmusson, E. M., and Carpenter, T. H., 1982: Variations in tropical sea surface temperature and surface wind fields associated with the Southern Oscillation/El Niño. *Monthly Weather Review*, **110**, 354-384.

Rasmusson, E. M., Wang, X., and Ropelewski, C., 1990: The biennial component of ENSO variability. *Journal of Marine Systems*, **1**, 71-96.

Read, J. F., and Gould, W. J., 1992: Cooling and freshening of the subpolar North Atlantic Ocean since the 1960s. *Nature*, **360**, 55-57.

Redmond, K. T., and Koch, R. W., 1991: Surface climate and streamflow variability in the western United States and their relationship to large-scale circulation indices. *Water Resources Research*, **27**, 2381-2399.

Richman, M. B., 1986: Rotation of principal components. *International Journal of Climatology*, **6**, 293-335.

Risbey, J. S., and Entekhabi, D., 1996: Observed Sacramento Basin streamflow response to precipitation and temperature changes and its relevance to climate impact studies. *Journal of Hydrology*, **184**, 209-224.

Rogers, J. C., 1988: Precipitation variability over the Caribbean and tropical Americas associated with the Southern Oscillation. *Journal of Climate*, **1**, 172-182.

Ropelewski, C. F., and Halpert, M. S., 1987: Global and regional scale precipitation patterns associated with the El Niño/Southern Oscillation (ENSO). *Monthly Weather Review,* **115**, 2352-2362.

Ropelewski, C. F., and Halpert, M. S., 1989: Precipitation patterns associated with the high-index of the Southern Oscillation. *Journal of Climate*, **2**, 268-284.

Ropelewski, C. F., and Halpert, M. S., 1996: Quantifying Southern Oscillation-precipitation relationships. *Journal of Climate*, **9**, 1043-1059.

Schlosser, P., Bonisch, G., Rhein, M., and Bayer, R., 1991: Reduction of deepwater formation in the Greenland Sea during the 1980s: Evidence from tracer data. *Science*, **251**, 1054-1056.

Slack, J. R., and Landwehr, J. M., 1992: Hydro-climatic data network (HCDN): A U.S. Geological Survey streamflow data set for the United States for the study of climate variations, 1874-1988. *U.S. Geological Survey Open-File Report* 92-129, 193 pp.

Stocker, T. F., and Broecker, W. S., 1994: Observation and modeling of North Atlantic Deep Water formation and its variability: Introduction. *Journal of Geophysical Research*, **99**, 12317.

Tanimoto, Y., Iwasaka, N., Hanawa, K., and Toba, Y., 1993: Characteristic variations of SST with multiple time scales in the North Pacific. *Journal of Climate*, **6**, 1153-1160.

Trenberth, K. E., 1984: Signal versus noise in the Southern Oscillation. *Monthly Weather Review*, **112**, 326-332.

Trenberth, K. E., 1990: Recent observed interdecadal climate changes in the Northern Hemisphere. *Bulletin, American Meteorology Society*, **71**, 988-993.

Trenberth, K. E., and Hoar, T. J., 1996: The 1990-1995 El Niño-Southern Oscillation event: Longest on record. *Geophysical Research Letters*, **23**, 57-60.

Trenberth, K. E., and Shea, D. J., 1987: On the evolution of the Southern Oscillation. *Monthly Weather Review*, **115**, 3078-3096.

Troup, A. J., 1965: The 'southern oscillation'. *Quarterly Journal of the Royal Meteorological Society,* **91**, 490-506.

Waylen, P. R., Quesada, M. E., and Caviedes, C. N., 1994: The effects of El Niño-Southern Oscillation on precipitation in San Jose, Costa Rica. *International Journal of Climatology*, **14**, 559-568.

Xie, P., and Arkin, P. A., 1996: Analyses of global monthly precipitation using gauge observations, satellite estimates and model predictions. *Journal of Climate*, **9**, 840-858.

Zhang, Y., Wallace, J. M., and Battisti, D. S., 1997: E NSO-like interdecadal variability: 1900-93. *Journal of Climate,* **10**,1004-1020.

Zorn, M. R., and Waylen, P. R., 1997: Seasonal response of mean monthly streamflow to El Niño/ Southern Oscillation in North Central Florida. *The Professional Geographer*, **49**, 51-62.